1   **Modulation of *Prdm9*-controlled meiotic chromosome asynapsis overrides**

2   **hybrid sterility in mice**

3

4   Sona Gregorova[1,§], Vaclav Gergelits[1,§], Irena Chvatalova[1,3], Tanmoy

5   Bhattacharyya[1,4], Barbora Valiskova[1,2], Vladana Fotopulosova[1], Petr Jansa[1], Diana

6   Wiatrowska[1], Jiri Forejt[1¶]

7

8   [1]Institute of Molecular Genetics, Academy of Sciences of the Czech Republic,

9   Division BIOCEV, Průmyslová 595, 252 50 Vestec, Czech Republic; [2]Charles

10 University, Faculty of Science, Albertov 2038/6, 128 00, Prague 10, Czech Republic.

11

12 Present address: [3]The National Institute of Public Health, Šrobárova 48, 100 42,

13 Prague 10, Czech Republic; [4]The Jackson Laboratory, 600 Main Street | Bar Harbor,

14 ME 04609, USA

15

16 [§]These authors contributed equally to this work

Abstract

The infertility of hybrids between closely related species is one of the reproductive isolation mechanisms leading to speciation. *Prdm9*, the only known vertebrate hybrid sterility gene causes failure of meiotic chromosome synapsis and infertility in male hybrids between mouse strains derived from two mouse subspecies. Within species *Prdm9* determines the sites of programmed DNA double-strand breaks and meiotic recombination hotspots. To investigate the relation between *Prdm9*-controlled meiotic arrest and asynapsis, we inserted random stretches of consubspecific homology on several autosomal pairs in sterile hybrids and analyzed their ability to form synaptonemal complexes and rescue male fertility. Twenty-seven or more Mb of consubspecific homology fully restored synapsis in a given autosomal pair and we predicted that two symmetric DSBs or more per chromosome are necessary for successful meiosis. We hypothesize that impaired recombination between evolutionary diverged homologous chromosomes could function as one of the mechanisms of hybrid sterility occurring in various sexually reproducing species.

32

Acknowledgments

45

Introduction

Hybrid sterility (HS) is a postzygotic reproductive isolation mechanism that safeguards speciation by restricting gene flow between related taxa. HS is a universal phenomenon observed in many eukaryotic inter-species hybrids, including yeast, plants, insects, birds, and mammals (COYNE and ORR 2004; MAHESHWARI and BARBASH 2010). In the early days of genetics, HS had been difficult to accommodate in Darwin's theory of evolution by natural selection until the Bateson - Dobzhansky - Muller incompatibility (BDMI) hypothesis (MULLER and PONTECORVO 1942; DOBZHANSKY 1951; ORR 1996) explicated HS and, more generally, any hybrid incompatibility, as a consequence of the independent divergence of mutually interacting genes and resulting aberrant interaction of the new alleles, previously not tested by natural selection. HS has several common features across various sexually reproducing eukaryotic species. Haldane's rule posits that if one sex of the F1 offspring of two different animal races is absent, rare, or sterile, it is the heterogametic sex (XY or ZW) (HALDANE 1922). Another common feature refers to the disproportionately large role of Chr X compared to autosomes in reproductive isolation (PRESGRAVES 2008). More recently, interaction between selfish genomic elements causing meiotic drive and their suppressors has been implicated in some instances of reproductive isolation (ORR 2005; ZHANG *et al.* 2015)

The molecular mechanisms underlying HS remain an unresolved question. Historically, genic and chromosomal mechanisms of HS were hypothesized, but the latter were soon dismissed as unlikely on the grounds that large chromosomal rearrangements do not segregate with HS genetic factors (DOBZHANSKY 1951). Other possible forms of non-genic chromosomal HS were not considered because of the

4

70 limited knowledge of the carrier of genetic information at the time. Thus, for the last

71 80 years or so, the focus on the genic control of HS prevailed (DOBZHANSKY 1951;

72 ORR 1996; FORSDYKE 2017). In studies mapping HS genes, the *Drosophila* group of

73 species has been the model of choice, yet only five *Drosophila* HS genes, namely

74 *OdsH*, *JYAlpha*, *Ovd*, *agt,* and *Taf1*, have been identified so far, none of which has a

75 known interacting gene predicted by the BDMI hypothesis (TING *et al.* 1998; MASLY *et*

76 *al.* 2006; PHADNIS and ORR 2009). The low success rate of the positional cloning of

77 HS genes was explained by the oligogenic or polygenic nature of HS phenotypes and

78 by the inherent difficulty in genetically dissecting the phenotype that prevents its own

79 transfer to progeny.

80 Over forty years ago, we introduced the house mouse (*Mus musculus*) as a

81 mammalian model for the genetic analysis of HS. The first HS locus *Hst1* was

82 genetically mapped in crosses of laboratory inbred strains (predominantly of *Mus*

83 *musculus domesticus* (*Mmd*) origin) with wild *Mus musculus musculus* (*Mmm*) mice

84 (FOREJT and IVANYI 1974). Later, we developed PWD/Ph and PWK/Ph inbred strains

85 purely from the wild *Mmm* mice of Central Bohemia (GREGOROVA and FOREJT 2000)

86 and used them in the positional cloning of *Hst1* by high-resolution genetic crosses

87 and physical mapping (GREGOROVA *et al.* 1996; TRACHTULEC *et al.* 1997). Finally, we

88 identified the *Hst1* locus with the PR domain containing 9 gene (*Prdm9*) (MIHOLA *et al.*

89 2009), coding for histone H3 lysine 4/lysine 36 methyltransferase (POWERS *et al.*

90 2016) the first and still the only HS gene known in vertebrates. Most of the tested

91 laboratory inbred strains share either the $Prdm9^{Dom2}$ or $Prdm9^{Dom3}$ allele. (PARVANOV

92 *et al.* 2010; BRUNSCHWIG *et al.* 2012). The former allele was found in inbred strains

93 producing sterile male hybrids when crossed with PWD females, while the $Prdm9^{Dom3}$

94   was observed in the strains that yielded quasi-fertile males in the same type of inter-

95   subspecific crosses (FOREJT *et al.* 2012).

96   The male sterility of (PWD x C57BL/6)F1 (henceforth PB6F1) hybrids depends on the

97   interaction of the heterozygous allelic combination $Prdm9^{Msc}/Prdm9^{Dom2}$ with the

98   PWD allelic form of the X-linked Hybrid sterility X chromosome 2, $Hstx2^{Msc}$ locus

99   (DZUR-GEJDOSOVA *et al.* 2012; BHATTACHARYYA *et al.* 2014). For the sake of clarity

100   and to stress the origin of the alleles we will use $Prdm9^{PWD}$, $Prdm9^{B6}$ and $Hstx2^{PWD}$ in

101   the rest of this paper. Any other tested allelic combination of these two major HS

102   genes yields fully fertile or subfertile male hybrids (DZUR-GEJDOSOVA *et al.* 2012;

103   FLACHS *et al.* 2012). The proper allelic combination of *Prdm9* and *Hstx2* genes is

104   necessary but not sufficient to completely govern HS because less than 10% instead

105   of expected 25% of (PWD x B6) x B6 male backcross progeny replicated the infertility

106   of male PB6F1 hybrids (DZUR-GEJDOSOVA *et al.* 2012). Initially, we explained this

107   'missing heritability' by assuming additional genic interaction of three or more

108   additional HS genes with a small effect that escaped the genetic screen (DZUR-

109   GEJDOSOVA *et al.* 2012). However, an alternative, non-genic explanation emerged

110   from the analysis of meiotic phenotypes of sterile hybrids. The failure of multiple

111   autosomal pairs to synapse properly, the persistence of phosphorylated histone

112   γH2AX indicating unrepaired DNA double-strand breaks (DSBs) on unsynapsed

113   chromosomes, and the disturbed transcriptional inactivation of sex chromosomes at

114   the first meiotic prophase were the most prominent features observed in

115   approximately 90% of primary spermatocytes of infertile PB6F1 inter-subspecific

116   hybrids (BHATTACHARYYA *et al.* 2013; BHATTACHARYYA *et al.* 2014). We suggested that

117   the failure of chromosomes to synapse could be related to their fast-evolving

118   nongenic DNA divergence. Because failure of proper synapsis in pachytene

6

119   spermatocytes is known to interfere with the normal progression of the first meiotic

120   division (MAHADEVAIAH *et al.* 2008; BURGOYNE *et al.* 2009), we assumed that the

121   asynapsis could be the ultimate cause of the sterility of male hybrids. Recently, the

122   role of PRDM9 zinc finger domain binding sites within noncoding genomic DNA has

123   been demonstrated in PB6F1 male HS. Replacement of the mouse sequence

124   encoding the PRDM9 zinc-finger array with the orthologous human sequence

125   reversed sterility in (PWD x B6-*Prdm9^{Hu}*)F1 hybrid males (DAVIES *et al.* 2016). In

126   PB6F1 hybrids, roughly 70% of *Prdm9*-directed DSBs hotspots identified by the

127   DMC1 ChIP-seq method were enriched on the 'nonself' homologous chromosome,

128   since the DSBs determined by the B6 allele of *Prdm9* were found predominantly or

129   exclusively on PWD chromosomes, and *vice versa*. Such hotspots were designated

130   as asymmetric DSB hospots. Chromosome-specific quantification of asymmetry

131   correlated well with the asynapsis rate across five arbitrarily chosen chromosomes of

132   PB6F1 hybrids (DAVIES *et al.* 2016; SMAGULOVA *et al.* 2016). Another, non-exclusive

133   interpretation of DMC1 ChIP-seq data pointed to significant enrichment of PRDM9-

134   independent hotspots in the PB6F1 hybrid testis, which occurs in promoters and

135   other regulatory motifs and which is characteristic of spermatogenic arrest in *Prdm9*

136   knockout males (SMAGULOVA *et al.* 2016). Recently, one third of PRDM9-dependent

137   DSBs was reported within sequences that have at least some repetitive character

138   and indicating that inappropriately high DSB levels in retroposons and other repetitive

139   elements may contribute to the infertility seen in some mouse hybrids (YAMADA *et al.*

140   2017).

141   In this work, we studied the relationship between meiotic chromosome asynapsis,

142   intersubspecific heterozygosity and male HS in a series of PB6F1 hybrids carrying

143   recombinant chromosomes with *Mmm/Mmm* consubpecific (belonging to the same

7

144 subspecies) PWD/PWD homozygous intervals on *Mmm/Mmd* intersubpecific

145 (belonging to different subspecies) PWD/B6 heterozygous background. We report

146 the restoration of synapsis of intersubspecific chromosome pairs in the presence of

147 27 Mb or more of consubspecific sequence, and the reversal of HS by targeted

148 suppression of asynapsis in the four most asynapsis-sensitive chromosomes. Thus

149 the asymmetry of PRDM9 hotspots is linked to failure of synapsis of homologous

150 chromosomes and to meiotic arrest of sterile hybrid males.

151

Results

Small chromosomes are more susceptible to asynapsis in sterile F1 hybrids

154 First, we ascertained the frequency of meiotic asynapsis separately for each

155 chromosome pair of PB6F1 hybrid males by combining fluorescence in-situ

156 hybridization (FISH) to decorate chromatin from individual chromosomes with

157 immunostaining of the synaptonemal complex protein 3 (SYCP3) a major component

158 of axial/lateral elements to visualize synaptonemal complexes, and a HORMA

159 domain-containing protein-2, HORMAD2 (WOJTASZ *et al.* 2012), to identify the axial

160 elements of unsynapsed chromosomes (*figure supplement 1A*). Altogether 4168

161 pachynemas from 40 PB6F1 hybrid males were analyzed. All autosomes of hybrid

162 males displayed a certain degree of asynapsis, classified as complete, partial, or

163 intermingled, with frequencies ranging from 2.6% (Chr 1) to 42.2% (Chr 19) (*Figure*

164 *1A - table supplement 1*). A strong bias was evident towards higher asynapsis rates

165 in the five smallest autosomes ($P < 5.3 \times 10^{-14}$, comparison of GLMM models, *Figure*

166 *1A)*. Recently, SPO11 oligos released during the processing of DSBs were

167   sequenced, mapped and quantified at chromosome-wide scale in male mice of the

168   B6 laboratory inbred strain (LANGE et al. 2016). This information, together with the

169   estimated frequency of asymmetric DSB hotspots in PBF1 hybrids (DAVIES et al.

170   2016; SMAGULOVA et al. 2016) enabled us to calculate the possible correlation

171   between the number of symmetric DSBs per chromosome and synapsis between

172   intersubspecific homologs. The calculation is based on and limited by the following

173   premises: (i) the overall densities of DSBs on individual chromosomes of B6 and

174   PB6F1 hybrid males are similar, (ii) approximately 250 DSBs occur per

175   leptotene/zygotene cell (KAUPPI et al. 2013), and (iii) the 0.28 proportion of symmetric

176   DSB hotspots in (PWD x B6)F1 hybrid males (DAVIES et al. 2016) is constant in all

177   autosomes. Under these conditions, a strong negative correlation (Spearman's ρ=-

178   0.76, P = 0.0002) of asynapsis rate with symmetric DSB hotspots (LANGE et al. 2016)

179   can be seen (*Figure 1B - table supplement 2*). This correlation is stronger than the

180   correlation of the asynapsis rate with the chromosomal physical length (Spearman's

181   ρ=-0.68, P = 0.0013). Importantly, the asynapsis rate cannot be better explained by

182   the chromosomal length (P = 0.709, comparison of GLMM models), when it is

183   controlled for the symmetric DSB hotspots (SPO11 oligos), while it is better explained

184   by the symmetric DSB hotspots (SPO11 oligos) when controlled for chromosomal

185   length (P = 0.046, comparison of GLMM models). Thus our findings indicate that

186   synapsis of a pair of homologous chromosomes depends on the presence of a

187   certain minimum number of symmetric DSB hotspots.

188   **Asynapsed chromosomes are devoid of active euchromatin**

189   The Cot-1 euchromatin RNA (ecRNA) is localized throughout the active interphase

190   chromosome territory *in cis* and does not diffuse into the rest of the nucleus like other

191   types of RNAs. EcRNA is mainly composed of repeat-rich noncoding RNA in active,

192   open euchromatin (HALL *et al.* 2014). Accordingly, we used Cot-1 DNA as a probe for

193   ecRNA FISH to compare the ecRNA distribution in asynapsed and synapsed

194   chromosomes. Pachytene spermatocytes of PB6F1 hybrids were examined for

195   subnuclear localization of active chromatin and asynapsed chromosomes using

196   confocal fluorescence microscopy after Cot-1 RNA FISH and HORMAD2

197   immunolabeling. Fluorescence signal quantification revealed that subnuclear regions

198   of asynapsed chromosomes composed of sex chromosomes and/or autosomal

199   univalents were lacking active euchromatin in contrast to other regions of the

200   pachytene nuclei (*Figure supplement 1B - video supplement 1*). We propose that the

201   absence of active euchromatin is a consequence of the meiotic synapsis failure of

202   intersubspecific chromosomes, known as meiotic silencing of unsynapsed chromatin

203   (MSUC (BURGOYNE *et al.* 2009)), which can act as an epigenic component

204   contributing to the meiotic phenotypes of sterile hybrids. Our findings are in

205   agreement with the transcriptional under-expression of genes on several autosomes

206   and disruption of meiotic sex chromosome inactivation (MSCI) in leptotene/zygotene

207   spermatocytes from semi-sterile *Mmm* x *Mmd* male hybrids with *Prdm9*$^{PWK/LEWES}$ and

208   *Hstx2*^{PWK} *or Hstx2*^{LEWES} allelic combinations (LARSON *et al.* 2016).

209   **The minimal length of consubspecific sequence necessary to rescue meiotic**

210   **chromosome synapsis**

211   We have shown previously that meiotic asynapsis affects intersubspecific (PWD/B6)

212   but not consubspecific (PWD/PWD) pairs of homologous chromosomes in sterile

213   male hybrids from crosses of PWD females and B6.PWD-Chr # consomic males

214   (GREGOROVA *et al.* 2008; BHATTACHARYYA *et al.* 2013). Here, we searched for the

215   minimum length of the PWD/PWD consubspecific sequence that still could secure

216   synapsis of a chromosome and potentially restore fertility in the hybrids. Instead of

10

217   substituting the whole PWD chromosome for its B6 homolog, we generated

218   recombinant PWD/B6 and B6/PWD (centromere/telomere) chromosomes. To do that,

219   we crossed the male hybrids between two B6.PWD-Chr# consomic strains and a

220   PWD female to match the intact maternal PWD homologs and estimated the

221   minimum size and location of consubspecific PWD/PWD stretches needed for

222   synapsis rescue as shown in *Figure 2A*. In three such generated 'two-chromosome

223   crosses' (hereafter 2-chr cross) we investigated the effect of the PWD/PWD

224   consubspecific intervals on the asynapsis rate in six different chromosomes - two in a

225   given experiment, namely Chr 5 & Chr 12 (*Figure 2B - table supplement 3 and 4*),

226   Chr 7 & Chr 15 (*Figure 2B - table supplement 5 and 6*) and Chr 17 & Chr 18 (*Figure

227   2B - table supplement 7 and 8*). Altogether over 12,000 pachynemas from 122

228   chromosomes were examined. All male progeny of the 2-chr crosses were fully

229   sterile, with low testis weight and the absence of sperm in the epididymis. The

230   analysis of data from six recombinant chromosomes revealed the following common

231   features:

232   - Introduction by recombination of 27 Mb or more of a consubspecific (PWD/PWD)

233   interval into a pair of intersubspecific (PWD/B6) homologs effectively suppressed the

234   asynapsis rate below the baseline of 5 % in all six studied autosomes (*Figure 2B).*

235   The efficiency of synapsis rescue was gradual with an apparent change point (*Figure

236   2B*). To describe the pattern in the data a segmented regression model was used

237   (see Materials and Methods). The model based on the data pooled from all 2-chr

238   crosses was selected as the best model with an estimated change point estimate at

239   27.14 Mb (19.36; 34.91) (95% CI) (see *table supplement 9*). The slope of the

240   decrease of asynapsis in the region of consubspecific intervals shorter than 27.14 Mb

11

241 was different for the respective chromosomes, reflecting the asynapsis rate in

242 respective chromosomes in F1 cross (P < 3 × 10^{-11} F-test).

243 - In spite of the known role of subtelomeric (bouquet) association in chromosome

244 pairing (ISHIGURO *et al.* 2014; SCHERTHAN *et al.* 2014), the location of the

245 consubspecific sequence at the telomeric end was not essential for synapsis. The

246 PWD/PWD intervals of sufficient size located at the centromeric (proximal), interstitial,

247 or telomeric (distal) positions rescued synapsis as well (*Figure 2B - table*

248 *supplements 3-8*).

249 **Reversal of hybrid sterility by targeted suppression of asynapsis of four of the most**

250 **asynapsis-sensitive autosomes**

251 The above experiments have shown that a randomly located consubspecific

252 PWD/PWD interval with a 27 or more Mb on otherwise intersubspecific PWD/B6

253 background is sufficient to restore the pachytene synapsis of a given autosomal pair.

254 To check the causal relationship between meiotic chromosome asynapsis and HS,

255 we attempted to reverse HS by reducing the asynapsis in the four most asynapsis-

256 prone chromosomes. Provided that hybrid male sterility is directly dependent on

257 chromosome synapsis we predicted, by multiplying the probabilities of the synapsis

258 of individual chromosomes obtained in F1 hybrids, that complete elimination of

259 asynapsis of four of the shortest autosomes (excluding Chr 17 to avoid *Prdm9*$^{PWD/PWD}$

260 interference) could increase the proportion of primary spermatocytes with the full set

261 of synapsed autosomes up to 26.7% and potentially abolish apoptosis of these cells

262 to yield around 5 million sperm cells in the epididymis of the hybrid males.

263 To evaluate the above prediction experimentally, random intervals of consomic Chrs

264 15^{PWD}, 16^{PWD}, 18^{PWD}, and 19^{PWD} were transferred on the genetic background of B6

265   mice in a three-generation cross as shown in *Figure 3A*. Eleven G3 males selected

266   for maximal extent of PWD sequence on these chromosomes were crossed to PWD

267   females (*Figure 3A -table supplement 10*). The resulting G4 hybrid male progeny

268   (hereafter 4-chr cross) displayed various degrees of PWD homozygosity in the

269   studied consomic autosomes on otherwise intersubspecific PWD/B6 genetic

270   background. As predicted, a significant fraction of hybrid males indeed showed

271   partial rescue of spermatogenesis. While in the PB6F1 cross, 100 % of hybrid males

272   displayed no sperm in the epididymis, in the 4-chr cross, only 51.7 % of 87 G4 males

273   were aspermic, 19.5 % had a 0.01–0.74 x 10^6 sperm count, and 28.7 % had 1.0–13.7

274   x 10^6 sperm cells (*Figure 3B - figure supplement 2, table supplement 11*).

275   Next, we asked whether the reversal of meiotic arrest correlates with the recovery of

276   meiotic synapsis of recombined chromosomes and with the size of PWD/PWD

277   consubspecific stretches in the four manipulated chromosomes. Eighteen G4 males

278   were deliberately selected according to their fertility parameters, 13 with HS partial

279   rescue, displaying sperm cells in the epididymis (0,1 x 10^6–6,9 x 10^6), and five

280   aspermic controls. The meiotic analysis of over 6500 pachynemas from the

281   genotyped males indeed confirmed the prediction based on the results of 2-chr

282   crosses. The nonrecombinant PWD/PWD consubspecific bivalents were always fully

283   synapsed, while all nonrecombinant PWD/B6 intersubspecific pairs revealed the

284   highest frequencies of asynapsis. All recombinant chromosomes with consubspecific

285   intervals of sufficient length (*Figure 3B -table supplement 12*; see *table supplement 9*

286   for change point estimates) effectively restored synapsis. Moreover, the presence of

287   sperm cells corresponded with the rescue of synapsis of consomic chromosomes. As

288   a rule of thumb, the hybrids had sperm when asynapsis was suppressed in at least

289   three of four segregating chromosomes and when the probability of all four consomic

290   chromosomes being synapsed was > 0.7. Chrs 16, 18, and 19 contributed the

291   strongest effect. (*Figure 3C - table supplement 12*).

Evidence for a trans-effect on the rate of asynapsis

293   Provided the probability of failure of the synapsis of each chromosome was

294   completely independent of the rest of the hybrid genome, the asynapsis rate of the

295   nonrecombinant intersubspecific chromosome pairs would be the same in F1 hybrids,

296   2-chr crosses, and 4-chr cross. Moreover, the frequency of pachynemas with all

297   chromosomes synapsed could be predicted from the observed frequencies of the

298   synapsis of individual chromosomes. Such predicted values would be close to the

299   values directly read from the meiotic spreads and would lie along the diagonal in

300   *Figure 4*. As shown below, both types of analysis clearly revealed that the asynapsis

301   rate of a particular chromosome depends on the synapsis status of other

302   chromosomes. In PB6F1 hybrids, the observed 13.1 % (11.4 %, 14.9 %) (95 % CI) of

303   fully synapsed pachynemas was double (P = 0.023, Mann-Whitney test) the rate

304   expected by the multiplication of the observed synapsis rates 6.6 % (5.3 %, 8.1 %) of

305   individual chromosomes (*Figure 4*) indicating a *trans* effect of synapsed autosomes

306   on the probability of the asynapsis of other intersubspecific chromosome pairs. The

307   tendency is more pronounced in data from 2-chr crosses and 4-chr cross

308   experiments. The most straightforward comparison is between the nonrecombinant

309   PWD/B6 intersubspecific chromosomes from F1 hybrids and 2-chr cross or 4-chr

310   crosses, where the asynapsis rate is dramatically reduced to 58–91 % of the

311   respective F1 hybrids' rates. Moreover, the difference between the observed and

312   expected ratios of asynaptic pachynemas increased with increasing probability of

313   sperm cells in the epididymis (*Figure 4 - table supplement 13*). In 4-chr cross, the

314   *trans* effect was analyzed further by comparing the asynapsis rate of a given

14

315   nonrecombinant PWD/B6 pair with the other three analyzed chromosomes. *Figure*

316   *supplement 3* shows a negative correlation (from r= -0.45 for Chr 16 to r = -0.88 for

317   Chr 15, linear regression slope is $\beta_{3\_chrs\_syn}$ = -0.19, P = 0.0003) between the

318   asynapsis rate of the nonrecombinant chromosome and the probability of synapsis of

319   the other three studied chromosomes.

320   It has to be emphasized that in the animals with identical *Prdm9* and *Hstx2* and

321   mostly intersubspecific chromosomes investigated in this work, the *cis*-effect of the

322   PWD/PWD length in a given chromosome dominates over the *trans*-effect. Namely,

323   the *trans*-effect can be more clearly observed when conditioned on the *cis*-effect of

324   the PWD/PWD length in a given chromosome (P = 0.002, F-test), while it is harder to

325   detect (P = 0.042, F-test) when the PWD/PWD length in a given chromosome is not

326   taken into account. On the other hand, the asynapsis rate critically depends on the

327   *cis*-effect of the PWD/PWD length in a given chromosome (P < 2×10^{-16}, F-test) when

328   the *trans*-effect is not taken into account.

329   To conclude, the described *trans* effect enhances the probability of the successful

330   pairing of intersubspecific chromosomes in males with identical *Prdm9* and *Hstx2*.

331   The mechanism is unknown, but it is tempting to speculate that a rate-limiting step of

332   an anti-recombination mismatch repair machinery (SPIES and FISHEL 2015;

333   CHAKRABORTY and ALANI 2016) could be involved as elaborated in Discussion.

334   **Discussion**

335   While the genic control of HS and meiotic synapsis in PBF1 hybrids can be

336   demonstrated by complete restitution of fertility and meiotic pairing in males with

337   *Prdm9*$^{PWD/PWD}$ or *Prdm9*$^{PWD/B6Hu}$ genotypes and partial recovery in *Prdm9*$^{PWD/C3H}$

338   males (DZUR-GEJDOSOVA *et al.* 2012; BHATTACHARYYA *et al.* 2013; DAVIES *et al.* 2016),

339   a chromosome-autonomous nature of asynapsis became apparent in experiments

340   where PB6F1 hybrids carried a single pair of PWD/PWD consubspecific homologs.

341   The males remained sterile, but synapsis of the particular consubspecific pair was

342   completely restored (BHATTACHARYYA *et al.* 2013). Such regulation of meiotic

343   asynapsis in PBF1 hybrids can be explained by a combined effect of the

344   chromosome-autonomous interaction of homologs operating *in cis* and *Prdm9/Hstx2*

345   incompatibility operating *in trans*. Here we separated the non-genic chromosome

346   autonomous from genic control mechanisms by keeping the sterility-determining

347   allelic combination of the *Prdm9^{PWD}/Prdm9^{B6}* gene and *Hstx2^{PWD}* locus constant in all

348   crosses, while successively introgressing stretches of the PWD/PWD consubspecific

349   sequence into eight PWD/B6 intersubspecific autosomal pairs.

350   **The meiotic asynapsis rate correlates with the presumed paucity of symmetric DSBs**

351   **in individual chromosomes in sterile hybrids**

352   Davies and coworkers (DAVIES *et al.* 2016) found that the DNA-binding zinc finger

353   domain of PRDM9 molecule is responsible for sterility in PB6F1 hybrids. In the sterile

354   hybrids, most PRDM9^{PWD}-specific hotspots reside on B6 chromosomes and, *vice*

355   *versa*, most of the PRDM9^{B6} binding sites are activated on PWD chromosomes. This

356   asymmetry could be explained in part by erosion of the PRDM9 binding sites due to

357   preferential transmission to progeny of the mutated hotspots motifs (BOULTON *et al.*

358   1997; MYERS *et al.* 2010). In a parallel study, (SMAGULOVA *et al.* 2016) authors

359   identified a novel class of strong hotspots absent in PWD and B6 parents apparently

360   related to asymmetric hotspots described in (DAVIES *et al.* 2016). Moreover, *Prdm9-*

361   independent 'default' hotspots were particularly enriched in Chr X and we noticed that

362   percentage of these 'default' hotspots in autosomes correlates with the present data

16

363 on asynapsis rate in F1 hybrids (Spearman's ρ = 0.69, P = 0.0012). We assume

364 that these *Prdm9*-independent hotspots could represent the late-forming DSBs on

365 unsynapsed chromosomes and, as such, they may be a consequence rather than the

366 cause of meiotic asynapsis (see (KAUPPI *et al.* 2013).

367 We found that meiotic asynapsis affects each autosomal pair in PB6F1

368 intersubspecific hybrids at distinctively unequal rates, with shorter chromosomes

369 affected more often than the longer ones. A similar pattern of higher sensitivity of

370 smaller autosomes to the synapsis failure was observed in mice with lowered

371 dosages of SPO11 (KAUPPI *et al.* 2013) and consequent twofold DSB reduction. The

372 fact that the asynapsis rate of sterile F1 hybrids correlates better with SPO11-oligo

373 derived DSB density (inferred from B6 mouse strain data (LANGE *et al.* 2016) than

374 with the chromosome length brings the first experimental evidence for the idea

375 (DAVIES *et al.* 2016) linking the asynapsis in sterile PB6F1 hybrids to insufficient

376 number of symmetric DSB hotspots.

377 **Small stretches of consubspecific sequence restore the synapsis of intersubspecific**

378 **chromosomes**

379 Provided that a shortage of symmetric DSB hotspots (DAVIES *et al.* 2016) is the

380 ultimate cause of failure of meiotic synapsis of intersubspecific homologs, then by

381 exchanging the asymmetric hotspots for the symmetric ones the full synapsis could

382 be restored. To experimentally test this prediction, we constructed pairs of PWD/B6

383 intersubspecific homologs with stretches of PWD/PWD consubspecific intervals,

384 which by definition cannot carry asymmetric hotspots. We found that chromosomes

385 with 27 Mb or longer stretches of consubspecific PWD/PWD sequence always

386 rescued full synapsis in male hybrids between PWD females and consomic B6.PWD-

17

387   Chr # males. The position of the consubspecific interval along the chromosome was

388   not critical for synapsis rescue, in accordance with the finding that synaptonemal

389   complexes nucleate at multiple recombination sites in each chromosome (ZICKLER

390   and KLECKNER 2015; FINSTERBUSCH *et al.* 2016). We assume that the presence of

391   symmetric DSB hotspots within the PWD/PWD homozygous stretches exceeded the

392   threshold of a minimum number of symmetric DSBs thus rescuing normal meiotic

393   synapsis.

394   Allowing for the assumptions enumerated in in the first section of Results the number

395   of DSBs necessary for proper synapsis of a given chromosome can be estimated

396   based on the expected distribution of symmetric DSB hotspots on all autosomes and

397   their asynapsis ratios in sterile F1 hybrids (*Table supplement 2*). We aimed to model

398   how the induction and repair of DSBs influence proper meiotic synapsis, and tried to

399   estimate the minimum number of symmetric DSBs per chromosome sufficient for full

400   meiotic synapsis. Our model predicts that in approximately 25 % of cases, a

401   chromosome is asynapsed because there is no symmetric DSB (median of

402   P(asynapsis) / P(0 symmetric DSBs) = 4.5). Assuming a critical threshold of the

403   required DSBs, the remaining 75 % of asynapsis could occur on chromosomes with

404   one symmetric DSB. It is consistent with our data that all asynapsis occurs when

405   there is 0 or 1 symmetric DSBs (median of P(asynapsis) / P(0 or symmetric DSBs) =

406   1.0) and that two symmetric DSBs per chromosome could be sufficient for full

407   development of the synaptonemal complex, as shown in *Figure 5* for PB6F1 hybrids.

408   The same conclusion also holds true for 2-chr cross and 4-chr cross experiments

409   (*Figure 5 - figure supplement 4 and 5*). The deviations from the diagonal in the

410   *Figure 5* depicting 4-chr cross can be explained by the *trans*-effect described in the

411   Results section.

On the chromosomal nature of hybrid sterility

412   It has been tacitly assumed, that the early meiotic arrest in sterile PBF1 males is due

413

414   to the high incidence of asynapsed chromosomes in zygotene/pachytene

415   spermatocytes of PBF1 hybrid males (BHATTACHARYYA *et al.* 2013). Here we provided

416   the first experimental evidence on linkage between *Prdm9*-controlled asynapsis and

417   meiotic arrest in PBF1 hybrid males by targeted suppression of asynapsis rate in

418   selected autosomes. The suppression of asynapsis in any of three combinations of

419   two PWD/B6 recombinant chromosomes (2-chr cross experiment) did not improve

420   the spermatogenic arrest. However, when hybrid genomes with four short

421   recombinant chromosomes (that are most sensitive to asynapsis) were constructed,

422   almost 50 % of males had sperm in the epididymis and normal testis size. By

423   improving synapsis in three of the four manipulated chromosomes (representing

424   ~11 % of the genome) with randomly located PWD/PWD homozygous intervals,

425   more than 40 % of pachynemas regained full chromosome synapsis and yielded

426   sperm. These results show that the high incidence of primary spermatocytes with

427   asynaptic chromosomes is indeed the factor determining the extent of meiotic arrest

428   in intersubspecific PBF1 hybrids.

429   The specific feature of PBF1 hybrid sterility consists in the inter-homolog interactions

430   controlled by the *Prdm9* and *Hstx2* genes. The interhomolog incompatibility caused

431   by single nucleotide variation in PRDM9 binding sites, which are situated away from

432   coding genes (BAUDAT *et al.* 2013) is proposed to make the asymmetric sites difficult

433   to repair (SMAGULOVA *et al.* 2016). We hypothesize that building the meiotic barrier

434   between (sub)species begins with genome-wide accumulation of single nucleotide

435   variants within PRDM9 binding sites and leading to gene conversion-guided meiotic

436 drive (BAKER *et al.* 2015). In the subspecific hybrids the asymmetric binding sites can

437 be more difficult to repair using the homolog from the other subspecies as a template

438 because of the strict requirements for sequence identity resulting in the rejection of

439 mismatched heteroduplex intermediates as demonstrated in yeast (SUGAWARA *et al.*

440 2004). Originally, such an inter-species barrier was proposed by Radman and

441 colleagues (RAYSSIGUIER *et al.* 1989; STAMBUK and RADMAN 1998) to prevent

442 homeologous recombination between *E. coli* and *Salmonella typhiimurium*. Among

443 eukaryotes, the role of the mismatch repair system in reproductive isolation was

444 reported in *Saccharomyces* species (HUNTER *et al.* 1996; GREIG *et al.* 2003; LITI *et al.*

445 2006). An exciting possibility arises that the heteroduplex rejection activity of

446 mismatch repair machinery could operate as a mechanism gradually restricting gene

447 flow between related (sub)species, a *conditio sine qua non* of speciation.

Materials and Methods

448

449 **Mice, Ethics Statement and Genotyping.** The mice were maintained at the Institute

450 of Molecular Genetics in Prague and Vestec, Czech Republic. The project was

451 approved by the Animal Care and use Committee of the Institute of Molecular

452 Genetics AS CR, protocol No 141/2012. The principles of laboratory animal care,

453 Czech Act No. 246/1992 Sb., compatible with EU Council Directive 86/609/EEC and

454 Apendix of the Council of Europe Convention ETS, were observed. SSLP markers

455 used for genotyping consomic chromosomes in 2-chr crosses and 4-chr cross are

456 listed in *table supplement 14*. Detailed descriptions of inbred mouse strains, fertility

457 testing and genotyping are given in the *Supplementary text.*

458 **Antibodies for the immunostaining of spread spermatocytes.** Detailed

459 descriptions of the preparation of meiotic spreads and the visualization of SYCP3,

460   γH2AFX, and HORMAD2 proteins on spreads of meiotic cells are given in the

461   *Supplementary Materials and Methods.*

462   **DNA and RNA FISH.** To identify individual chromosomes, XMP Xcyting Mouse

463   Chromosome N Whole Painting Probes (Metasystem) were used for DNA FISH.

464   Identification of nascent RNA in pachytene spermatocytes was performed as

465   previously described (MAHADEVAIAH *et al.* 2009), with modifications. A detailed

466   description is given in the *Supplementary Materials and Methods.*

467   **Microscopy and image capture**. Images were observed using a Nikon Eclipse 400

468   epifluorescence microscope and captured with a DS-QiMc mono-chrome camera

469   (Nikon). Images were analyzed using the NIS elements program. A detailed

470   description is given in the *Supplementary Materials and Methods.*

471   **Statistics**

472   All calculations were performed in the statistical environment R 3.2.2. For modeling

473   the dependence between the asynapsis rate and the number of symmetric DSBs, we

474   determined the probabilistic distribution of the number of symmetric DSBs. The

475   distribution was determined by simulation and with parameters based on previous

476   studies: (i) The number of DSBs per cell (BHATTACHARYYA *et al.* 2013) was modeled

477   as an observation from the normal distribution N(250, sd=20). (ii) We assumed a

478   number of DSBs proportional to Spo11 oligos (LANGE *et al.* 2016) in each autosome.

479   (iii) The positions of DSBs in the particular autosome were simulated from the

480   uniform distribution, U(0, Autosome length). (iv) For the intersubspecific part of the

481   autosome, the number of symmetric DSBs was simulated from the binomial

482   distribution Bi(n=N_DSBs_in_het_part, p=0.28 (DAVIES *et al.* 2016; SMAGULOVA *et al.*

483   2016) For the consubspecific part of the autosome, all DSBs were taken as

21

484 symmetric. The total number of symmetric DSBs in the autosome was taken as the

485 sum of symmetric DSBs in the respective parts.

486 Steps (i) - (iv) were performed in N=100000 simulations to obtain a probabilistic

487 distribution. Further details on statistical evaluation are given in the *Supplementary*

488 *Materials and Methods.*

489

490 _____

References

492 BAKER, C. L., S. KAJITA, M. WALKER, R. L. SAXL, N. RAGHUPATHY *et al.*, 2015 PRDM9
493   drives evolutionary erosion of hotspots in Mus musculus through haplotype-
494   specific initiation of meiotic recombination. PLoS Genet **11:** e1004916.

495 BAUDAT, F., Y. IMAI and B. DE MASSY, 2013 Meiotic recombination in mammals:
496   localization and regulation. Nat Rev Genet **14:** 794-806.

497 BHATTACHARYYA, T., S. GREGOROVA, O. MIHOLA, M. ANGER, J. SEBESTOVA *et al.*, 2013
498   Mechanistic basis of infertility of mouse intersubspecific hybrids. Proc Natl
499   Acad Sci U S A **110:** E468-477.

500 BHATTACHARYYA, T., R. REIFOVA, S. GREGOROVA, P. SIMECEK, V. GERGELITS *et al.*,
501   2014 X chromosome control of meiotic chromosome synapsis in mouse inter-
502   subspecific hybrids. PLoS Genet **10:** e1004088.

503 BOULTON, A., R. S. MYERS and R. J. REDFIELD, 1997 The hotspot conversion paradox
504   and the evolution of meiotic recombination. Proc Natl Acad Sci U S A **94:**
505   8058-8063.

506 BRUNSCHWIG, H., L. LEVI, E. BEN-DAVID, R. W. WILLIAMS, B. YAKIR *et al.*, 2012 Fine-
507   scale maps of recombination rates and hotspots in the mouse genome.
508   Genetics **191:** 757-764.

509 BURGOYNE, P. S., S. K. MAHADEVAIAH and J. M. TURNER, 2009 The consequences of
510   asynapsis for mammalian meiosis. Nat Rev Genet **10:** 207-216.

511 COYNE, J. A., and H. A. ORR, 2004 *Speciation*. Sinauer Associates, Sunderland,
512   Massachusetts.
513 DAVIES, B., E. HATTON, N. ALTEMOSE, J. G. HUSSIN, F. PRATTO *et al.*, 2016 Re-
514   engineering the zinc fingers of PRDM9 reverses hybrid sterility in mice. Nature
515   **530:** 171-176.
516 DOBZHANSKY, T., 1951 in *Genetics and the origin of Species*. Columbia University,
517   New York.
518 DZUR-GEJDOSOVA, M., P. SIMECEK, S. GREGOROVA, T. BHATTACHARYYA and J. FOREJT,
519   2012 Dissecting the genetic architecture of f(1) hybrid sterility in house mice.
520   Evolution **66:** 3321-3335.
521 FINSTERBUSCH, F., R. RAVINDRANATHAN, I. DERELI, M. STANZIONE, D. TRANKNER *et al.*,
522   2016 Alignment of Homologous Chromosomes and Effective Repair of
523   Programmed DNA Double-Strand Breaks during Mouse Meiosis Require the
524   Minichromosome Maintenance Domain Containing 2 (MCMDC2) Protein.
525   PLoS Genet **12:** e1006393.
526 FLACHS, P., O. MIHOLA, P. SIMECEK, S. GREGOROVA, J. C. SCHIMENTI *et al.*, 2012
527   Interallelic and intergenic incompatibilities of the Prdm9 (Hst1) gene in mouse
528   hybrid sterility. PLoS Genet **8:** e1003044.
529 FOREJT, J., and P. IVANYI, 1974 Genetic studies on male sterility of hybrids between
530   laboratory and wild mice (Mus musculus L.). Genet Res **24:** 189-206.
531 FOREJT, J., J. PIALEK and Z. TRACHTULEC, 2012 Hybrid male sterility genes in the
532   mouse subspecific crosses, pp. 482-503 in *Evolution of the House Mouse*,
533   edited by M. MACHOLAN, S. J. E. BAIRD, P. MUCLINGER and J. PIALEK.
534   Cambridge University Press, Cambridge.
535 FORSDYKE, D. R., 2017 Speciation: Goldschmidt's chromosomal heresy, once
536   supported by Gould and Dawkins, is again reinstated. Biol. Theory **12:** 4-12.
537 GREGOROVA, S., P. DIVINA, R. STORCHOVA, Z. TRACHTULEC, V. FOTOPULOSOVA *et al.*,
538   2008 Mouse consomic strains: exploiting genetic divergence between Mus m.
539   musculus and Mus m. domesticus subspecies. Genome Res **18:** 509-515.
540 GREGOROVA, S., and J. FOREJT, 2000 PWD/Ph and PWK/Ph inbred mouse strains of
541   Mus m. musculus subspecies--a valuable resource of phenotypic variations
542   and genomic polymorphisms. Folia Biol (Praha) **46:** 31-41.

543 GREGOROVA, S., M. MNUKOVA-FAJDELOVA, Z. TRACHTULEC, J. CAPKOVA, M. LOUDOVA *et*
544 *al.*, 1996 Sub-milliMorgan map of the proximal part of mouse Chromosome 17
545 including the hybrid sterility 1 gene. Mamm Genome **7:** 107-113.

546 GREIG, D., M. TRAVISANO, E. J. LOUIS and R. H. BORTS, 2003 A role for the mismatch
547 repair system during incipient speciation in Saccharomyces. J Evol Biol **16:**
548 429-437.

549 HALDANE, J., 1922 Sex ration and unisexual sterility in animal hybrids. J. Genet. **12:**
550 101-109.

551 HALL, L. L., D. M. CARONE, A. V. GOMEZ, H. J. KOLPA, M. BYRON *et al.*, 2014 Stable
552 C0T-1 repeat RNA is abundant and is associated with euchromatic interphase
553 chromosomes. Cell **156:** 907-919.

554 HUNTER, N., S. CHAMBERS, E. LOUIS and R. BORTS, 1996 The mismatch repair system
555 contributes to meiotic sterility in an interspecific yeast hybrid. EMBO J **15:**
556 1726-1733.

557 CHAKRABORTY, U., and E. ALANI, 2016 Understanding how mismatch repair proteins
558 participate in the repair/anti-recombination decision. FEMS Yeast Res **16:** pii:

559 fow071.

560 ISHIGURO, K., J. KIM, H. SHIBUYA, A. HERNANDEZ-HERNANDEZ, A. SUZUKI *et al.*, 2014
561 Meiosis-specific cohesin mediates homolog recognition in mouse
562 spermatocytes. Genes Dev **28:** 594-607.

563 KAUPPI, L., M. BARCHI, J. LANGE, F. BAUDAT, M. JASIN *et al.*, 2013 Numerical
564 constraints and feedback control of double-strand breaks in mouse meiosis.
565 Genes Dev **27:** 873-886.

566 LANGE, J., S. YAMADA, S. E. TISCHFIELD, J. PAN, S. KIM *et al.*, 2016 The Landscape of
567 Mouse Meiotic Double-Strand Break Formation, Processing, and Repair. Cell
568 **167:** 695-708 e616.

569 LARSON, E. L., S. KEEBLE, D. VANDERPOOL, M. D. DEAN and J. M. GOOD, 2016 The
570 composite regulatory basis of the large X-effect in mouse speciation. Mol Biol
571 Evol **34:** 282-295.

572 LITI, G., D. B. H. BARTON and E. J. LOUIS, 2006 Sequence diversity, reproductive
573 isolation and species concepts in Saccharomyces. Genetics **174:** 839-850.

574 MAHADEVAIAH, S. K., D. BOURC'HIS, D. G. DE ROOIJ, T. H. BESTOR, J. M. TURNER *et al.*,
575 2008 Extensive meiotic asynapsis in mice antagonises meiotic silencing of

576   unsynapsed chromatin and consequently disrupts meiotic sex chromosome
577   inactivation. J Cell Biol **182:** 263-276.
578 MAHADEVAIAH, S. K., Y. COSTA and J. M. TURNER, 2009 Using RNA FISH to study
579   gene expression during mammalian meiosis. Methods Mol Biol **558:** 433-444.
580 MAHESHWARI, S., and D. A. BARBASH, 2010 The Genetics of Hybrid Incompatibilities.
581   Annu Rev Genet **45:** 331-355.
582 MASLY, J. P., C. D. JONES, M. A. NOOR, J. LOCKE and H. A. ORR, 2006 Gene
583   transposition as a cause of hybrid sterility in Drosophila. Science **313:** 1448-
584   1450.
585 MIHOLA, O., Z. TRACHTULEC, C. VLCEK, J. C. SCHIMENTI and J. FOREJT, 2009 A mouse
586   speciation gene encodes a meiotic histone H3 methyltransferase. Science
587   **323:** 373-375.
588 MULLER, H., and G. PONTECORVO, 1942 Recessive genes causing interspecific
589   sterility and other disharmonies between Drosophila melanogaster and
590   simulans. Genetics **27:** 157.
591 MYERS, S., R. BOWDEN, A. TUMIAN, R. E. BONTROP, C. FREEMAN *et al.*, 2010 Drive
592   against hotspot motifs in primates implicates the PRDM9 gene in meiotic
593   recombination. Science **327:** 876-879.
594 ORR, H. A., 1996 Dobzhansky, Bateson, and the genetics of speciation. Genetics
595   **144:** 1331-1335.
596 ORR, H. A., 2005 The genetic basis of reproductive isolation: insights from Drosophila.
597   Proc Natl Acad Sci U S A **102 Suppl 1:** 6522-6526.
598 PARVANOV, E. D., P. M. PETKOV and K. PAIGEN, 2010 Prdm9 controls activation of
599   mammalian recombination hotspots. Science **327:** 835.
600 PHADNIS, N., and H. A. ORR, 2009 A single gene causes both male sterility and
601   segregation distortion in Drosophila hybrids. Science **323:** 376-379.
602 POWERS, N. R., E. D. PARVANOV, C. L. BAKER, M. WALKER, P. M. PETKOV *et al.*, 2016
603   The Meiotic Recombination Activator PRDM9 Trimethylates Both H3K36 and
604   H3K4 at Recombination Hotspots In Vivo. PLoS Genet **12:** e1006146.
605 PRESGRAVES, D. C., 2008 Sex chromosomes and speciation in Drosophila. Trends
606   Genet **24:** 336-343.
607 RAYSSIGUIER, C., D. S. THALER and M. RADMAN, 1989 The barrier to recombination
608   between Escherichia coli and Salmonella typhimurium is disrupted in
609   mismatch-repair mutants. Nature **342:** 396-401.

610 SCHERTHAN, H., K. SCHOFISCH, T. DELL and D. ILLNER, 2014 Contrasting behavior of
611   heterochromatic and euchromatic chromosome portions and pericentric
612   genome separation in pre-bouquet spermatocytes of hybrid mice.
613   Chromosoma **123:** 609-624.

614 SMAGULOVA, F., K. BRICK, Y. M. PU, R. D. CAMERINI-OTERO and G. V. PETUKHOVA,
615   2016 The evolutionary turnover of recombination hot spots contributes to
616   speciation in mice. Genes & Development **30:** 266-280.

617 SPIES, M., and R. FISHEL, 2015 Mismatch repair during homologous and
618   homeologous recombination. Cold Spring Harb Perspect Biol **7:** a022657.

619 STAMBUK, S., and M. RADMAN, 1998 Mechanism and control of interspecies
620   recombination in Escherichia coli. I. Mismatch repair, methylation,
621   recombination and replication functions. Genetics **150:** 533-542.

622 SUGAWARA, N., T. GOLDFARB, B. STUDAMIRE, E. ALANI and J. E. HABER, 2004
623   Heteroduplex rejection during single-strand annealing requires Sgs1 helicase
624   and mismatch repair proteins Msh2 and Msh6 but not Pms1. Proc Natl Acad
625   Sci U S A **101:** 9315-9320.

626 TING, C., S. TSAUR, M. WU and C. WU, 1998 A rapidly evolving homeobox at the site
627   of a hybrid sterility gene [see comments]. Science **282:** 1501-1504.

628 TRACHTULEC, Z., M. MNUKOVA-FAJDELOVA, R. M. HAMVAS, S. GREGOROVA, W. E.
629   MAYER *et al.*, 1997 Isolation of candidate hybrid sterility 1 genes by cDNA
630   selection in a 1.1 megabase pair region on mouse chromosome 17. Mamm
631   Genome **8:** 312-316.

632 WOJTASZ, L., J. M. CLOUTIER, M. BAUMANN, K. DANIEL, J. VARGA *et al.*, 2012 Meiotic
633   DNA double-strand breaks and chromosome asynapsis in mice are monitored
634   by distinct HORMAD2-independent and -dependent mechanisms. Genes Dev
635   **26:** 958-973.

636 YAMADA, S., S. KIM, S. E. TISCHFIELD, M. JASIN, J. LANGE *et al.*, 2017 Genomic and
637   chromatin features shaping meiotic double-strand break formation and repair
638   in mice. Cell Cycle**:** 1-15.

639 ZHANG, L., T. SUN, F. WOLDESELLASSIE, H. XIAO and Y. TAO, 2015 Sex ratio meiotic
640   drive as a plausible evolutionary mechanism for hybrid male sterility. PLoS
641   Genet **11:** e1005073.

642 ZICKLER, D., and N. KLECKNER, 2015 Recombination, Pairing, and Synapsis of
643   Homologs during Meiosis. Cold Spring Harb Perspect Biol **7:** pii: a016626.

644

645
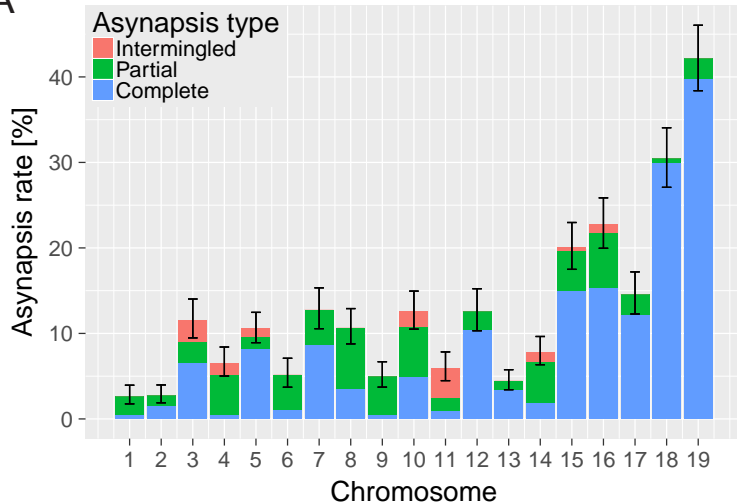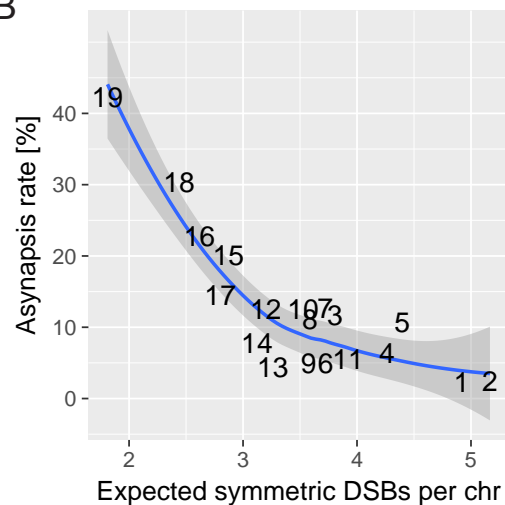
Figure 1. The asynapsis rate of individual autosomes in sterile male (PWD x B6)F1 hybrids. (*A*) Mean asynapsis rate ± S.E (based on GLMM model). Intermingled asynapsis refers to overlaps of two or more asynapsed chromosomes within the DNA FISH cloud of chromatin. Smaller chromosomes had higher asynapsis rate (GLMM model, $P < 1.1 \times 10^{-13}$). Concurrently, the chromosomes with higher asynapsis rate were also more involved in complete rather than partial asynapsis (GLMM model, $P < 6.3 \times 10^{-5}$). Proportion of complete and partial asynapsis was controlled by the asynapsis rate rather the chromosomal length (test for effect of the length when controlled for the asynapsis rate, 0.491). (*B*) Negative correlation (Spearman's ρ = -0.76, P = 0.0002) between asynapsis rate and mean expected number of symmetric DSBs (29) based on the chromosome-wide distribution of SPO11 oligos in fertile B6 males (30).

The following table supplement is available for figure 1.

Table supplement 1. Asynapsis rate of individual chromosomes of (PWD x B6)F1 males.
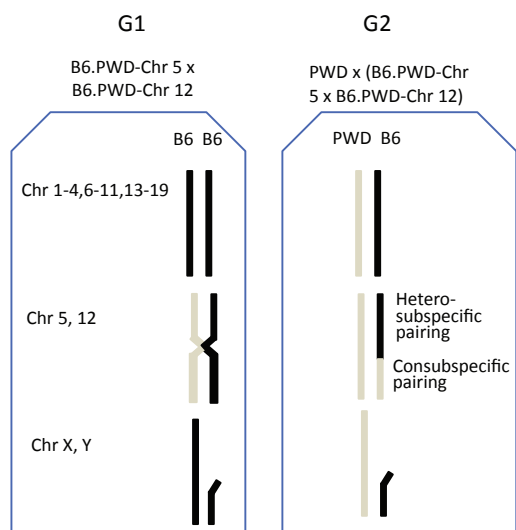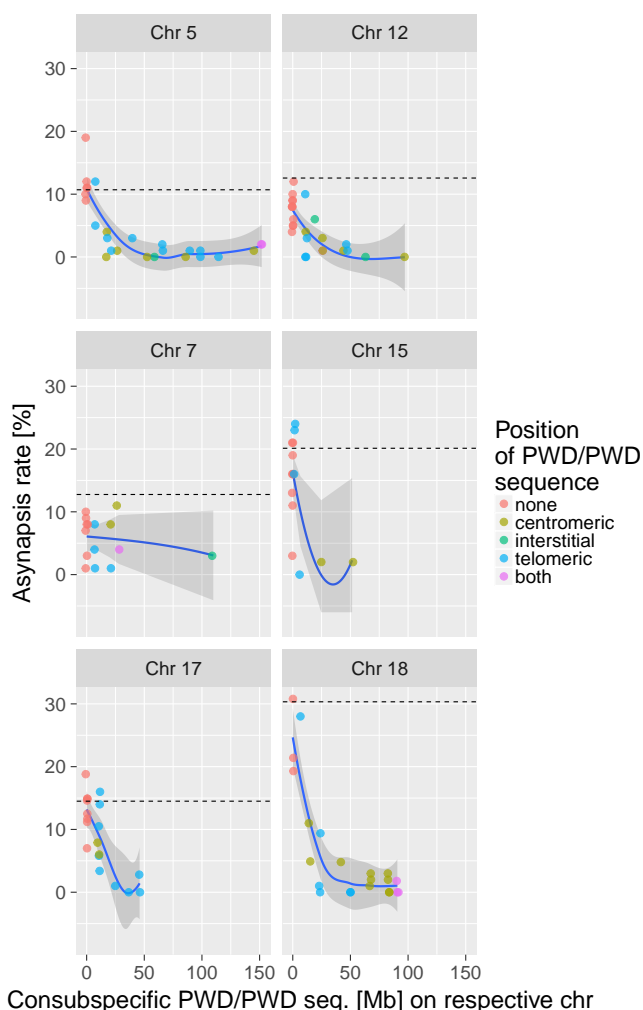
Figure 2. The effect of consubspecific PWD/PWD stretches of genomic sequence on pachytene synapsis, 2-chr cross. (*A*) The F1 hybrid males of two consomic strains (generation 1 - G1, Chr 5 and Chr 12 shown here) were crossed to PWD females to produce generation 2 - G2 sterile F1 hybrids with random recombinant consomic chromosomes 5 and 12. Using whole chromosome probes, the asynapsis rate of the consomic chromosomes was scored by DNA FISH. (*B*) Combination of two chromosomes (5+12, 7+15 and 17+18) were challenged in each experiment. The localization of PWD homozygous sequence with respect to centromere, interstitial part of the chromosome, telomere, or on both ends is distinguished by color (see also Tables Supplement 3 – Supplement 8). The average length between the minimum and maximum of the consubspecific sequence is plotted. The mean asynapsis rate of a given chromosome is regularly higher in PB6F1 hybrids (dashed line) than in 2-chr cross. For explanation see Fig. 4 and the chapter on the trans-effect dependent variation in asynapsis rate. Loess curve with 95% CI.

The following table supplements are available for figure 2.

Table supplement 3. The effect of the size and location of PWD/PWD consubspecific intervals on asynapsis of Chr 5.

Table supplement 4. The effect of the size and location of PWD/PWD consubspecific intervals on asynapsis of Chr 12.

Table supplement 5. The effect of the size and location of PWD/PWD consubspecific intervals on asynapsis of Chr 7.

Table supplement 6. The effect of the size and location of PWD/PWD consubspecific intervals on asynapsis of Chr 15.

Table supplement 7. The effect of the size and location of PWD/PWD consubspecific intervals on asynapsis of Chr 17.

Table supplement 8. The effect of the size and location of PWD/PWD consubspecific intervals on asynapsis of Chr 18.
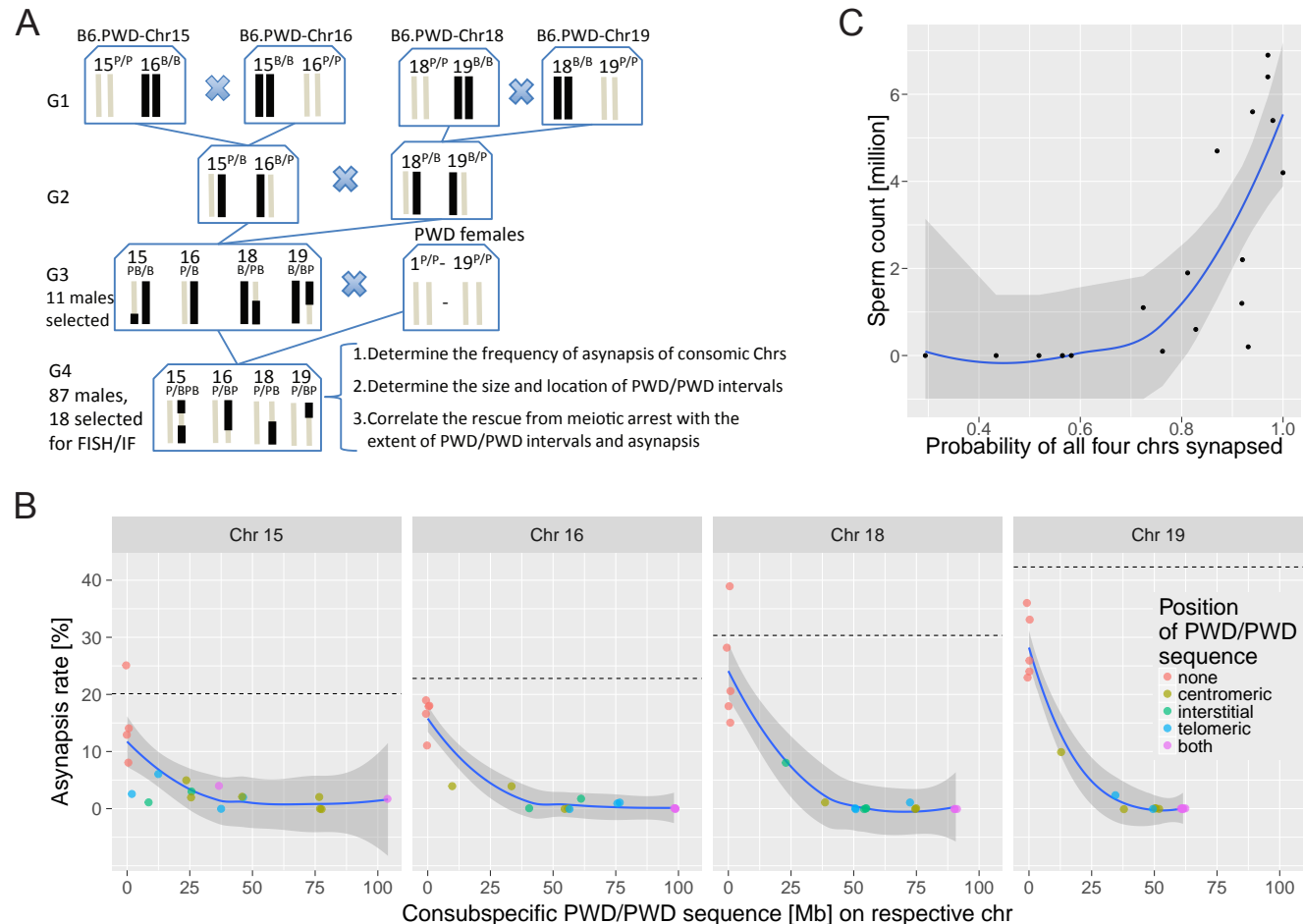
Figure 3. The effect of consubspecific PWD/PWD stretches of genomic sequence on pachytene synapsis and meiotic progression, 4-chr cross. (*A*) Scheme of a four-generation cross resulting in F1 hybrids with four recombinant consomic chromosomes. (*B*) The asynapsis rate related to the size and chromosomal position of the consubspecific PWD/PWD sequence in four consomic chromosomes (15, 16, 18 and 19, see also Table 1). The localization of PWD homozygous sequence with respect to centromere, interstitial part of the chromosome, telomere, or on both ends is distinguished by color (see also Tables 1). (*C*) Number of sperm in epididymis is a function of probability of synapsis of all four consomic chromosomes. The complete meiotic arrest is reversed in males having 70% or higher chance of all four chromosomes synapsed. See also Table Supplement 11. Loess curve with 95% CI.

The following table and figure supplements are available for figure 3.

Table supplement 9. Change point estimates of the minimal length [Mb] of PWD/PWD homozygosity showing detectable affect on synapsis rate.

Table supplement 10. Eleven G3 male parents selected for the 4-chr cross experiment.

Table supplement 11. The fertility parameters of hybrids of the 4-chr cross experiment.

Table supplement 12. Four-chr cross. The effect of the size and location of PWD/PWD consubspecific intervals on asynapsis of Chrs 15, 16, 18 and 19 and on fertility parameters.

Figure supplement 2. The fertility parameters of hybrids of the 4-chr cross experiment.
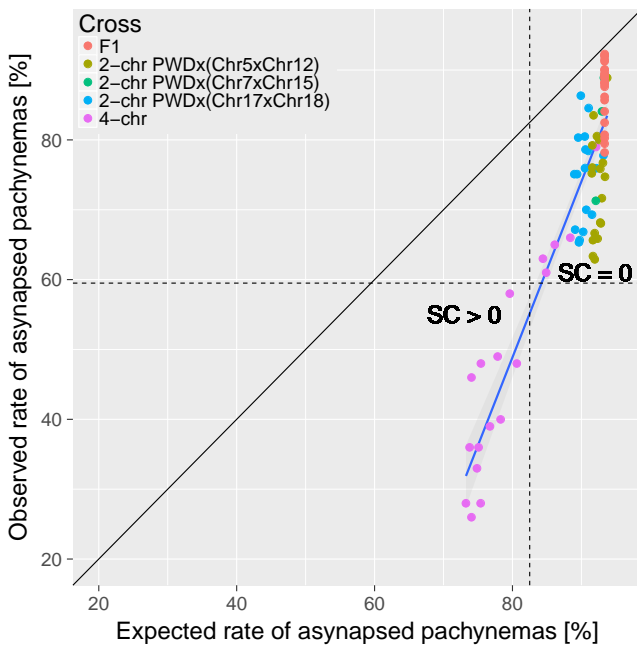
Figure 4. The trans-acting effect of consubspecific PWD/PWD stretches increases the probability of full synapsis of PWD/B6 heterosubspecific homologs in males 2-chr cross and 4-chr cross experiments. The expected rate of synapsed pachynemas was calculated for each mouse in 2-chr cross and 4-chr cross experiments by multiplication of observed synapsis rates (i.e. assuming independence) of FISH analyzed chromosomes (e.g. chrs 15, 16, 18 and 19 in 4-chr cross) and observed PB6F1 synapsis rates of the remaining autosomes. Asynapsis rate was calculated as a complement to synapsis rate. The difference between expected and observed overall asynapsis is most pronounced in 4-chr cross males with the lowest expected overall asynapsis rate. Recovery of spermatogenesis signaled by the presence of sperm in the epididymis occurs when more than 40% of pachynemas are fully synapsed. SC is sperm count.

The following table supplement is available for figure 4.

Table supplement 13. Four-chr cross experiment. The relation between observed and calculated rate of pachytene asynapsis and fertility parameters.
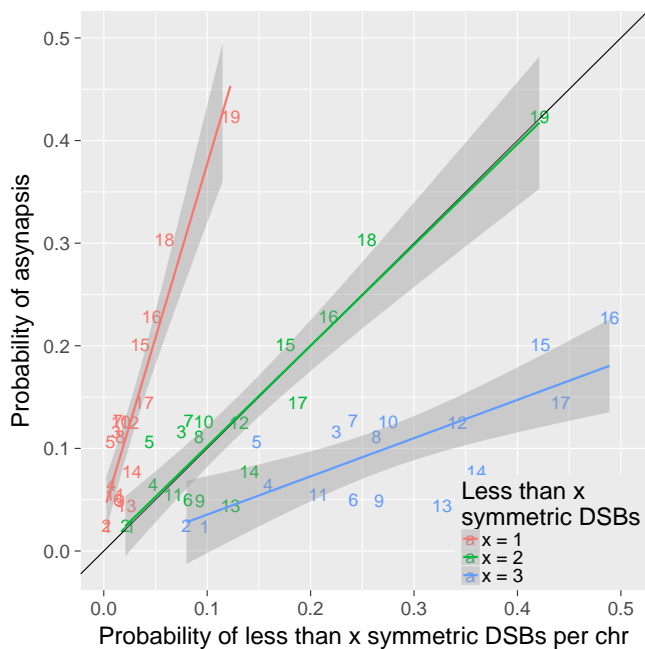
Figure 5. Two or more symmetric DSBs can be sufficient for synapsis. The probability of less than 1 symmetric DSBs per chromosome is ~4 times lower than the asynapsis rate observed in PB6F1 hybrid males, (i.e. estimate of probability of asynapsis) implying ~75% of all asynapsis occurs when there is 1 or more repairable DSBs. The probability of less than 2 symmetric DSBs is a good estimate of the probability of asynapsis, while the probability of less than 3 symmetric DSBs overestimates the probability of asynapsis. This shows that in the simplest explanation two or more symmetric DSBs could be sufficient for synapsis. The probabilistic distribution of symmetric DSBs is calculated based on the model described in the Discussion.

The following figure supplements are available for figure 5.

Figure supplement 4. Two and more symmetric DSBs can be sufficient for synapsis in 2-chr cross males. See Fig. 5 for details.

Figure supplement 5. Two or more symmetric DSBs can be sufficient for synapsis in 4-chr cross hybrid males. See Fig. 5 for details.

Supplementary Information for

Modulation of *Prdm9*-controlled meiotic chromosome asynapsis overrides hybrid sterility in mice

Sona Gregorova, Vaclav Gergelits, Irena Chvatalova, Tanmoy Bhattacharyya, Barbora Valiskova, Vladana Fotopulosova, Petr Jansa, Diana Wiatrowska, Jiri Forejt

This Supplementary Information contains the supplementary materials and methods, figure supplements and table supplements

Supplementary Materials and Methods

Mice, ethics statement. The project was approved by the Animal Care and use Committee of the Institute of Molecular Genetics AS CR, protocol No 141/2012. The principles of laboratory animal care, Czech Act No. 246/1992 Sb., compatible with EU Council Directive 86/609/EEC and Apendix of the Council of Europe Convention ETS, were observed. SSLP markers used for genotyping consomic chromosomes in 2-chr crosses and 4-chr cross are listed in Table supplement 14.

The PWD/Ph inbred strain originated from a single pair of wild mice of the *Mus musculus musculus* subspecies trapped in 1972 in Central Bohemia, Czech Republic (Gregorova and Forejt, 2000). The C57BL/6J (B6) inbred strain was purchased from The Jackson Laboratory. The panel of 27 chromosome substitution strains C57BL/6J-Chr #PWD (abbreviated B6.PWD-Chr #) was prepared in our laboratory and is maintained by the Institute of Molecular Genetics AS CR, Division BIOCEV, Vestec, Czech Republic, and by The Jackson laboratory, Bar Harbor, Maine, U.S.A. All mice were maintained in a 12-h light/12-h dark cycle in a specific pathogen-free barrier facility. The mice had ad libitum access to a standard rodent diet (ST-1, 3.4% fat; VELAZ) and water. All males were killed at age 60–70 d.

Immunostaining and image capture

For immunocytochemistry, the spread nuclei were prepared as described (Anderson et al. 1999) with modifications. Briefly, a single-cell suspension of spermatogenic cells in 0.1M sucrose with Protease inhibitors (Roche) was dropped on 1% paraformaldehyde-treated slides and allowed to settle for 3 hours in a humidified box at 4°C. After brief H_2O and PBS washing and blocking with 5% goat sera in PBS (vol/vol), the cells were immunolabeled using a standard protocol with the following antibodies: anti-HORMAD2 (1:700, rabbit polyclonal

antibody, gift from Attila Toth) and SYCP3 (1:50, mouse monoclonal antibody, Santa Cruz, #74569). Secondary antibodies were used at 1:500 dilutions and incubated at room temperature for 60 min; goat anti-Rabbit IgG-AlexaFluor568 (MolecularProbes, A-11036) and goat anti-Mouse IgG-AlexaFluor647 (MolecularProbes, A-21235). The images were acquired and examined in a Nikon Eclipse 400 microscope with a motorized stage control using a Plan Fluor objective, 60x (MRH00601; Nikon) and captured using a DS-QiMc monochrome CCD camera (Nikon) and the NIS-Elements program (Nikon). The images were processed using the Adobe Photoshop CS software (Adobe Systems).

Combined immunofluorescence staining with DNA FISH or RNA FISH

XMP XCyting Mouse Chromosome N Whole Painting Probes (Metasystems) were used for DNA FISH analysis of asynapsis of all autosomes, one at a time, as described (Turner et al. 2005), with slight modifications. Testes from 8-week-old mice were dissected and spread meiocyte nuclei were prepared as described previously (Mahadevaiah et al. 2009) with a modification, which relies on reversed sequence of RNA FISH and immunofluorescence staining (Turner et al. 2005). Briefly, after cell fixation and permeabilization, the immunofluorescent labeling was performed for 90 min at 20ºC with primary anti HORMAD2 and anti SYCP3 antibodies. Secondary antibodies were selected as above and incubated at room temperature for 60 min. After washing and postfixation steps, the immunostained nuclei were processed with RNA fluorescence in situ hybridization. The Cot-1 DNA biotin-labeled probe was incubated overnight at 37ºC, and then the hybridized biotinylated Cot-1 probe was labelled with FITC-avidin conjugate and the fluorescent signal was amplified as described previously (Chaumeil et al, 2008). The images of the immunofluorescence stained

and cot-1 RNA FISH-labeled spread spermatocytes were examined and photographed using confocal microscope DMI6000CEL – Leica TCS SP8.

Statistics

The effects of the number of Spo11 oligos and the chromosomal length on the asynapsis rate were investigated using a GLMM model. In all the used GLMM models in this work, the asynapsis was modeled as a binary response to fixed effects under investigation and a random intercept for each animal. In F1 hybrids 95 % confidence intervals of observed rate of asynapsed pachynemas and expected rated of asynapsed pachynemas were calculated by bootstrap. The estimates of mean asynapsis rate in respective chromosomes, their standard errors and 95 % confidence intervals were based on GLMM model. In 2-chr crosses and 4-chr cross 95 % confidence intervals of asynapsis rate were constructed based on the likelihood ratio to capture also the uncertainty in the cases when zero asynapsis rate per mouse and chromosome was observed.

Based on the nature of the dependence between the asynapsis rate and the length of consubspecific PWD/PWD region on chromosomes of 2-chr crosses and 4-chr cross, we fitted the data by segmented two-part continuous regression models (Vito et al. 2003)

We fitted the models for all the chromosomes separately (Table supplement 9) being aware of the limitations caused by the lack of animals having specific lengths of consubspecific PWD/PWD region in the respective chromosomes. As the best model describing the dependence of asynapsis rate on the lenghts of PWD/PWD intervals we selected piecewise linear models fitting 1) pooled data from 2-chr crosses and 2) pooled data from both 2-chr crosses and 4-chr cross. Those models are not severely affected by the lack of observations with specific lengths of PWD/PWD segment nor by outliers.

All calculations were performed in R 3.2.2, the change point models and GLMM models were fitted using the packages segmented and lme4, respectively (Vito et al. 2008, Douglas et al. 2015).

Gregorova S, Forejt J (2000) PWD/Ph and PWK/Ph inbred mouse strains of Mus m. musculus subspecies--a valuable resource of phenotypic variations and genomic polymorphisms. *Folia Biol (Praha)* **46:** 31-41

Anderson LK, Reeves A, Webb LM, Ashley T (1999) Distribution of crossing over on mouse synaptonemal complexes using immunofluorescent localization of MLH1 protein. *Genetics* 151(4):1569-1579.

Turner JM, Mahadevaiah SK, Fernandez-Capetillo O, NussenzweigA, Xu X, Deng CX, Burgoyne PS (2005) Silencing of unsynapsed meiotic chromosomes in the mouse. Nat Genet;37(1):41–47.

Chaumeil J, Augui S,Cow JC, and Heard E (2008) Combined immunofluorescence, RNA fluorescent in situ hybridization, and DNA fluorescent in situ hybridization to study chromatin changes, transcriptional activity, nuclear organization, and X-chromosome inactivation. Methods Mol Biol;463:297-308.

Mahadevaiah SK, Costa Y, Turner JM (2009) Using RNA FISH to study gene expression during mammalian meiosis. In: Keeney S (ed) Meiosis, vol volume 2, cytological methods. Methods in molecular biology. Humana, New York, pp 433–444.

Bhattacharyya T, *et al.* (2013) Mechanistic basis of infertility of mouse intersubspecific hybrids. *Proceedings of the National Academy of Sciences of the United States of America* 110(6):E468-477.

Lange J, *et al.* (2016) The Landscape of Mouse Meiotic Double-Strand Break Formation, Processing, and Repair. *Cell* 167(3):695-708 e616.29,

Davies B, *et al.* (2016) Re-engineering the zinc fingers of PRDM9 reverses hybrid sterility in mice. *Nature* 530(7589):171-+.

Smagulova F, Brick K, Pu YM, Camerini-Otero RD, & Petukhova GV (2016) The evolutionary turnover of recombination hot spots contributes to speciation in mice (vol 30, pg 266, 2016). *Genes & development* 30(7):871-871.

Vito MR, Muggeo (2003). Estimating regression models with unknown break-points. Statistics in Medicine, 22, 3055-3071.

Vito MR Muggeo (2008). Segmented: an R Package to Fit Regression Models with Broken-Line Relationships. R News, 8/1, 20-25. URL https://cran.r-project.org/doc/Rnews/.

Bates D, Maechler M, Bolker B, Walker S (2015). Fitting Linear Mixed-Effects Models Using lme4. Journal of Statistical Software, 67(1), 1-48.<doi:10.18637/jss.v067.i01>
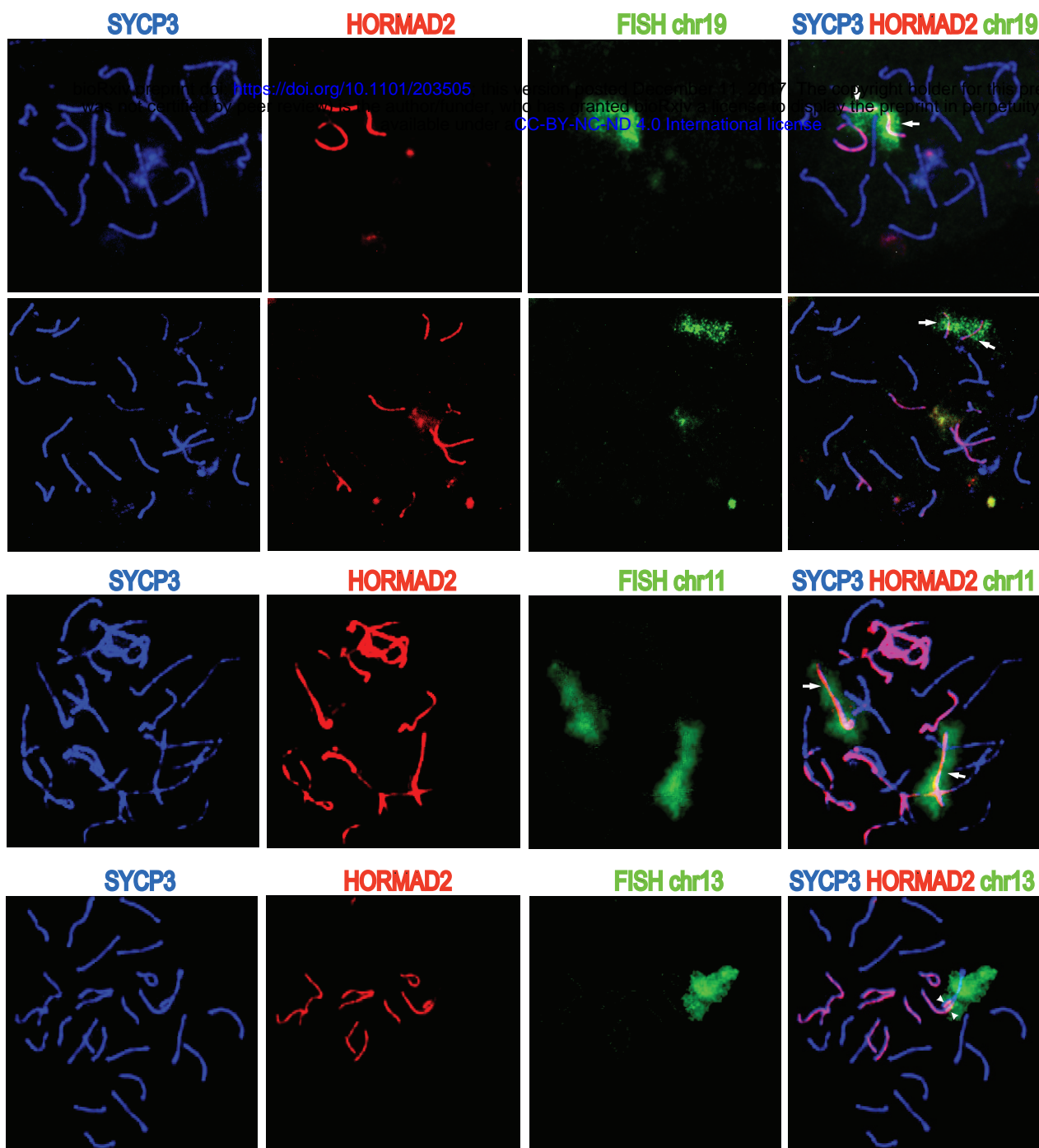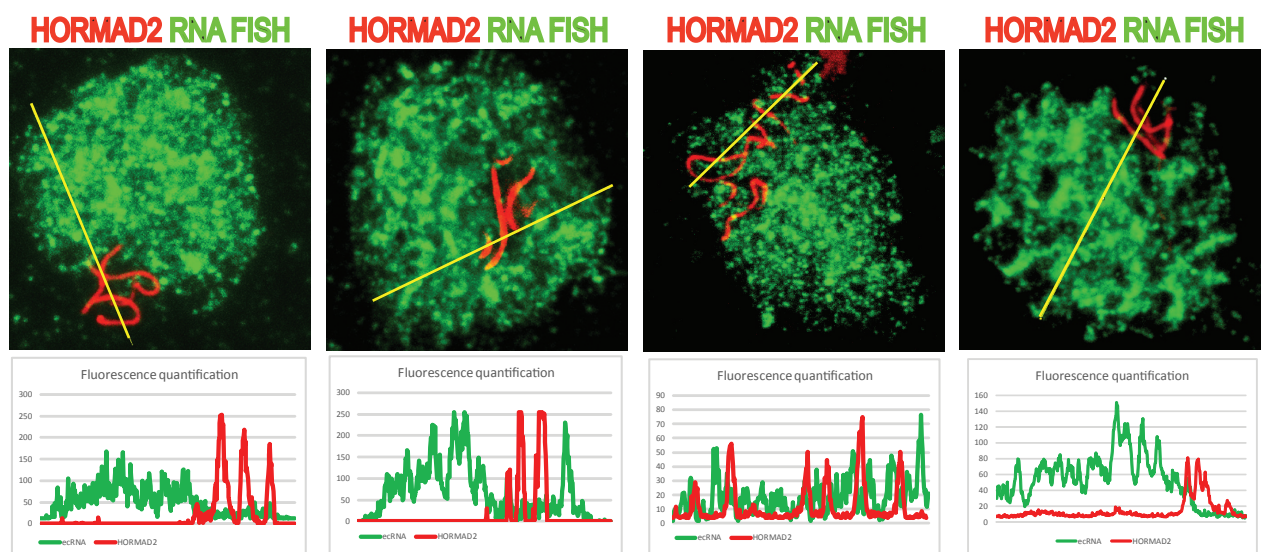
Figure supplement 1. Asynapsis of heterosubspecific homologs in PB6F1 pachynemas. (A) Partial (arrowheads) and complete (arrows) asynapsis of Chr 19, 11 and 13. HORMAD2-labeled chromosomes with synapsis defects often form tangles via nonhomologous pairing. (B) Asynapsed chromosomes are embedded in transcriptionally silenced chromatin visualized by the lack of ecRNA detected by Cot1 RNA FISH See also video 1.
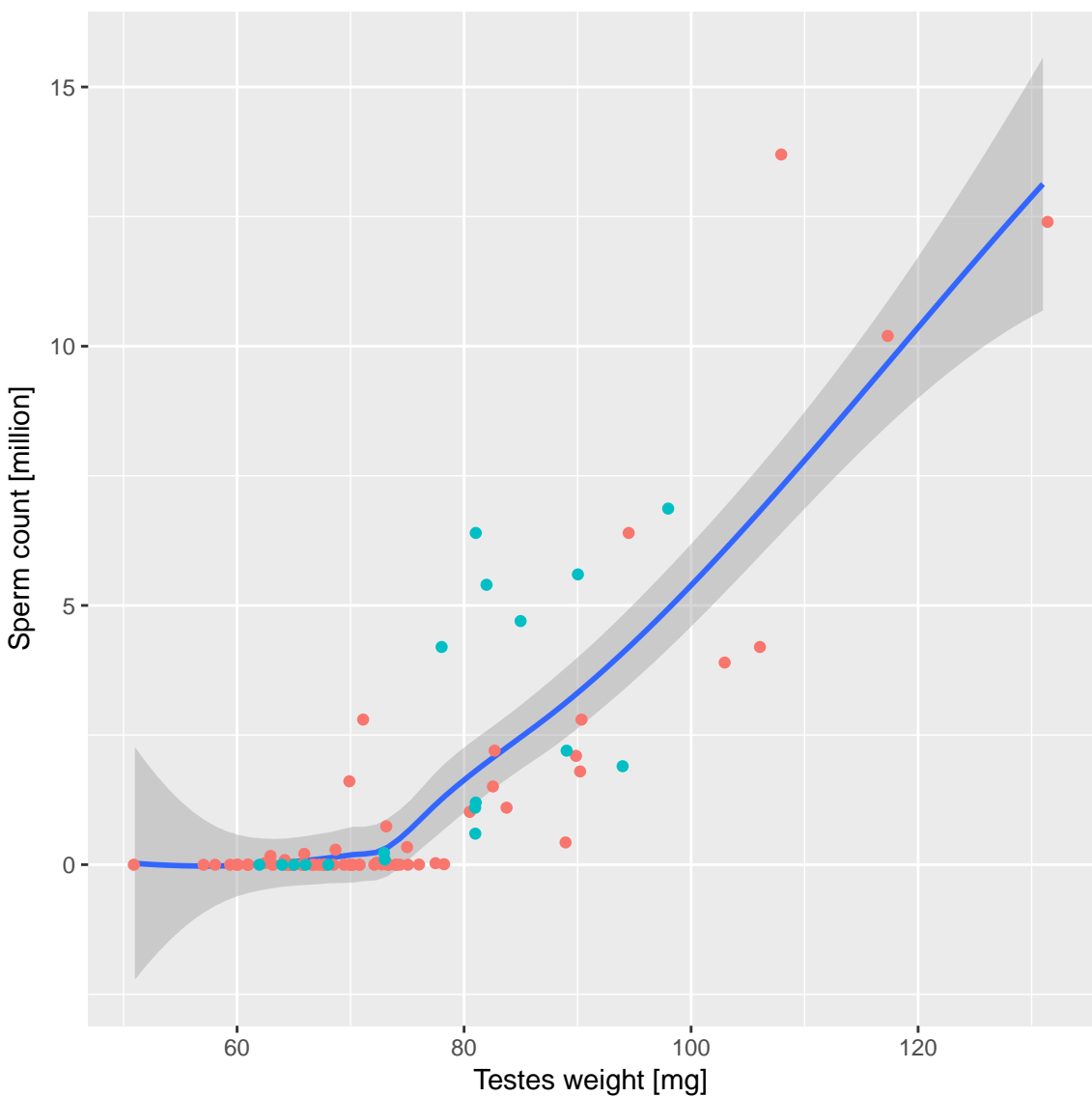
Figure supplement 2. Fertility parameters of G4 males from the 4-chr cross. Rescue of HS meiotic arrest is detectable in males with the weight of paired testes >70 mg and >0.1 x 10^6 of sperm in the epididymis. The males selected for DNA FISH/HORMAD2 analysis of asynapsis are highlighted in turquoise. All males share the sterility-determining allelic combination of *Prdm9*$^{PWD/B6}$ and *Hstx2*^{PWD}. Loess curve with 95% CI.
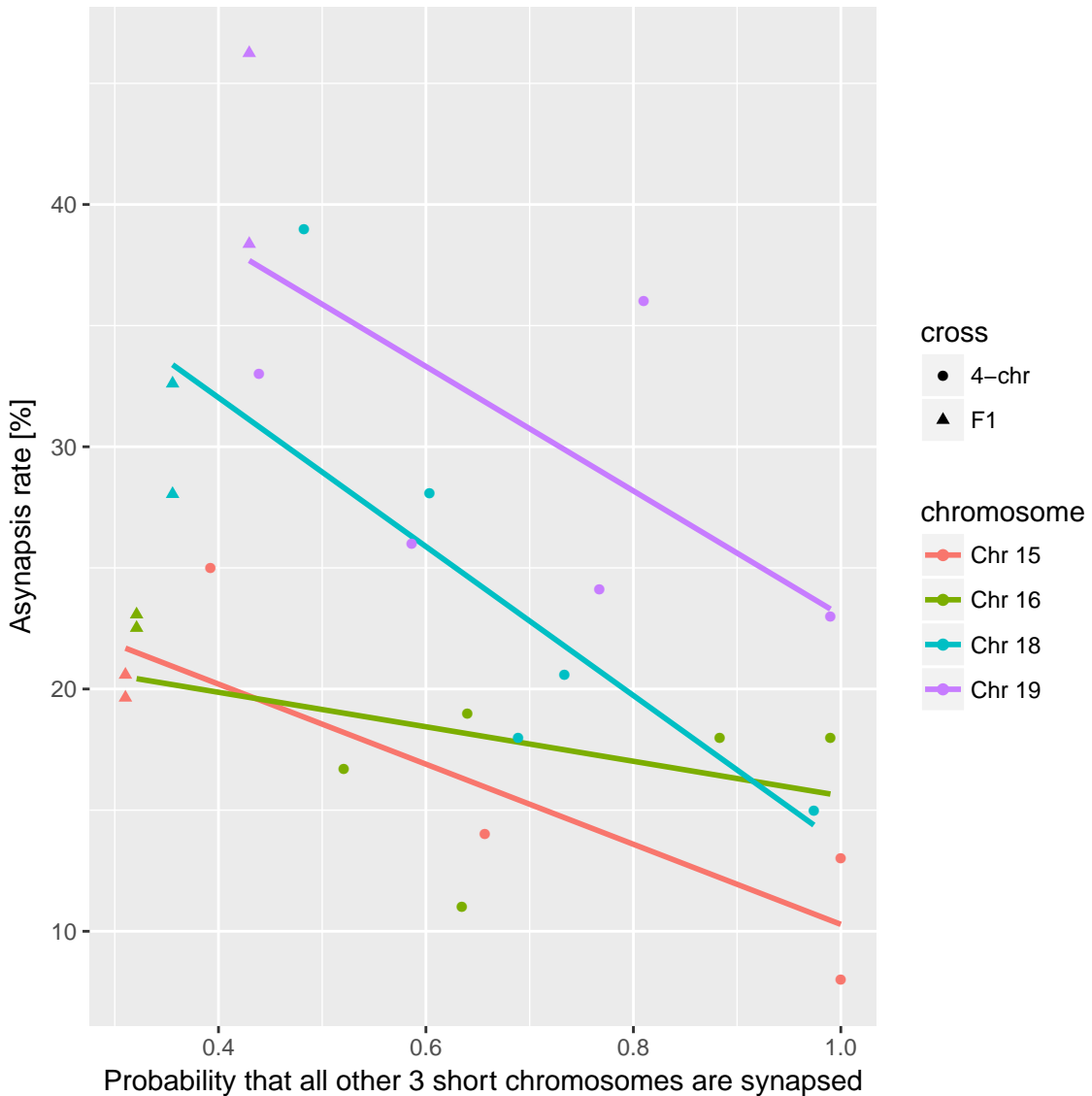
Figure supplement 3. Asynapsis rate of individual nonrecombinant consomic PWD/B6 chromosomes modified in trans by the probability of synapsis of the remaining 3 consomic chromosomes in 4-chr cross in individual males compared to PB6F1 hybrids. Asynapsis rate of a given chromosome is in negative correlation (r = -0.88, -0.45, -0.80, -0.67 for Chrs 15, 16, 18, 19 respectively) with the probability that all other 3 analyzed chromosomes are synapsed. The slope of linear regression is $\beta_{3\_chrs\_syn}$ = -0.19, overall P = 0.0003.
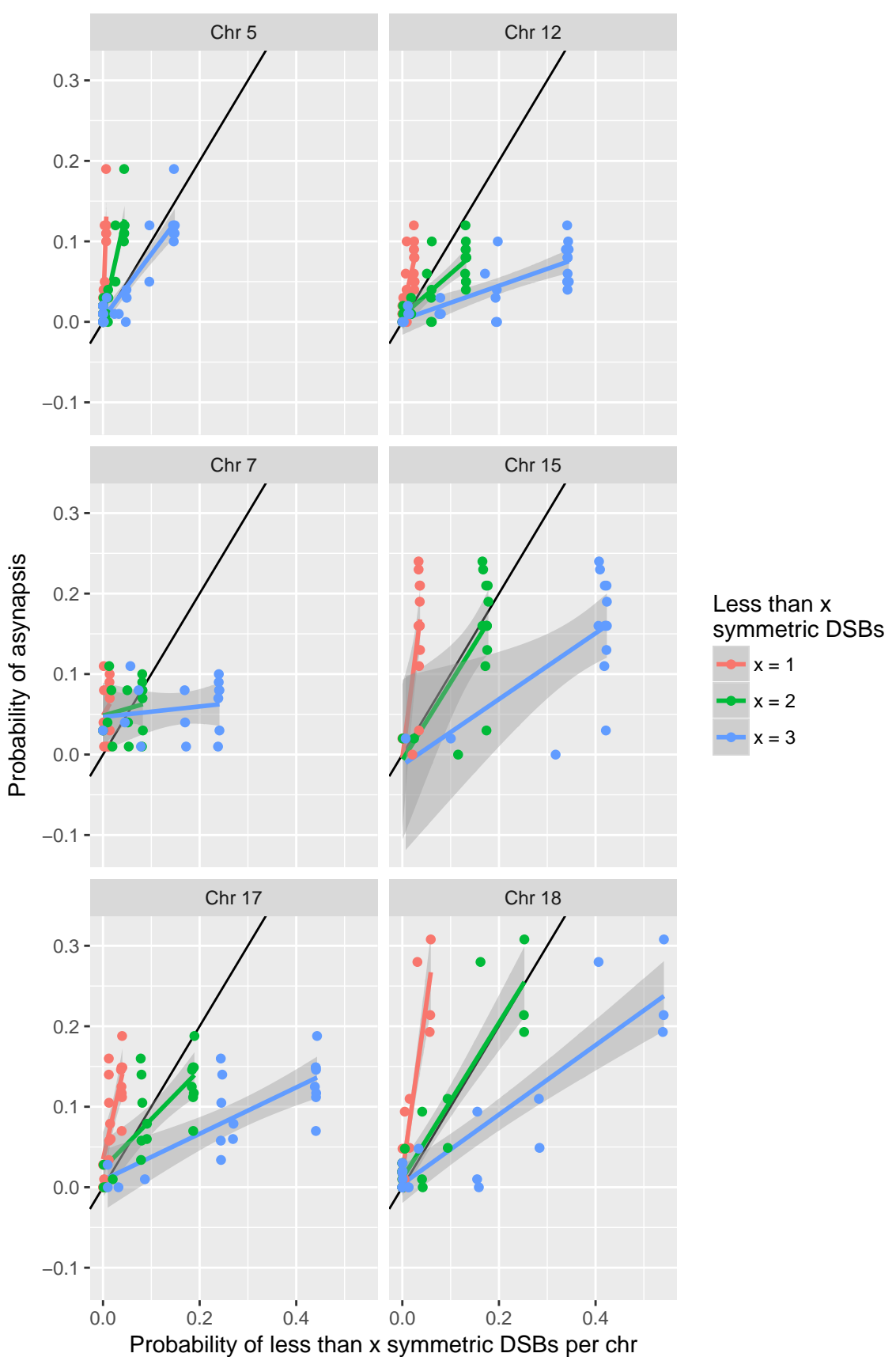
Figure supplement 4. Two and more symmetric DSBs can be sufficient for synapsis in 2-chr cross males. See Fig. 5 for details.
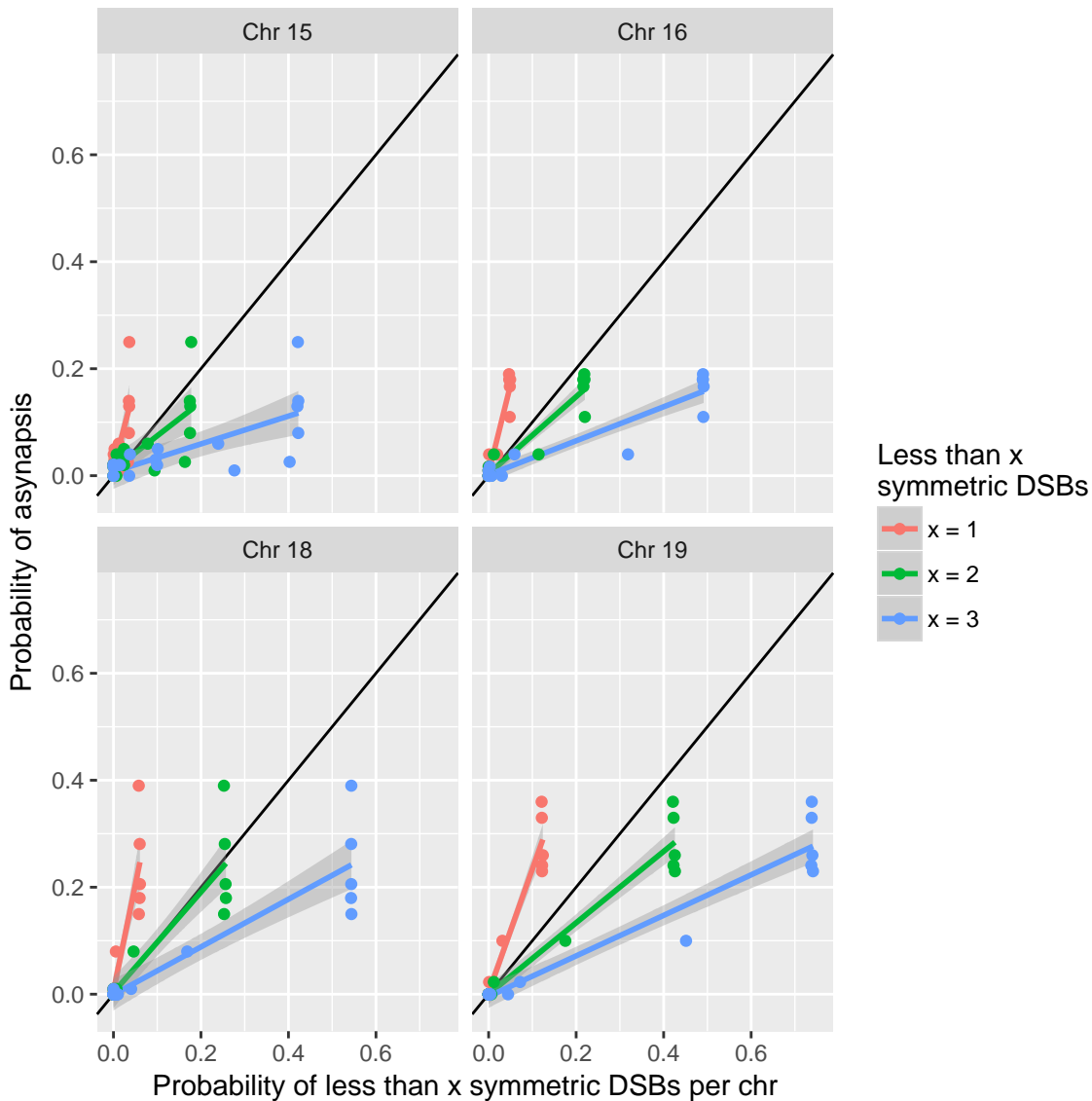
Figure supplement 5. Two or more symmetric DSBs can be sufficient for synapsis in 4-chr cross hybrid males. See Fig. 5 for details.

Table supplement 1. Asynapsis rate of individual chromosomes of (PWD x B6)F1 hybrid males

Chromosome	Asynapsis	Asynapsis	Synapsis	Complete Asynapsis	Partial Asynapsis	Intermingled Asynapsis	Number of Males per Chr	Analyzed cells	Comlete Asynapsis	Partial Asynapsis	Intermingled Asynapsis
Name	Mean [%]	95% CI	Mean [%]	Mean [%]	Mean [%]	Mean [%]	N	n, per male	n, per male	n, per male	n, per male
chr1	2,6	1.2; 5.8	97,4	0,4	2,2	0,0	2	125; 102	1; 0	5; 0	0; 0
chr2	2,7	1.3; 5.6	97,3	1,6	1,2	0,0	2	103; 152	1; 3	0; 3	0; 0
chr3	11,6	7.8; 16.8	88,4	6,5	2,5	2,5	2	81; 118	4; 9	2; 3	4; 1
chr4	6,5	3.9; 10.7	93,5	0,5	4,6	1,4	2	110; 105	1; 0	7; 3	2; 1
chr5	10,6	7.6; 14.6	89,4	8,3	1,3	1,0	3	85; 89; 129	6; 9; 10	0; 3; 1	0; 2; 1
chr6	5,1	2.7; 9.6	94,9	1,1	4,0	0,0	2	70; 105	1; 1	2; 5	0; 0
chr7	12,8	8.8; 18.2	87,2	8,7	4,1	0,0	2	94; 102	10; 7	2; 6	0; 0
chr8	10,7	7.3; 15.4	89,3	3,6	7,1	0,0	2	93; 132	3; 5	10; 6	0; 0
chr9	5,0	2.8; 8.8	95,0	0,5	4,5	0,0	2	107; 113	0; 1	3; 7	0; 0
chr10	12,6	8.8; 17.6	87,4	4,9	5,8	1,8	2	114; 109	8; 3	3; 10	2; 2
chr11	5,9	3.4; 10.2	94,1	1,0	1,5	3,5	2	126; 76	2; 0	2; 1	5; 2
chr12	12,6	8.5; 18.2	87,4	10,4	2,2	0,0	2	92; 91	10; 9	2; 2	0; 0
chr13	4,4	2.6; 7.4	95,6	3,5	1,0	0,0	3	112; 106; 97	3; 4; 4	2; 0; 1	0; 0; 0
chr14	7,8	5.2; 11.7	92,2	1,9	4,8	1,1	2	129; 139	4; 1	3; 10	0; 3
chr15	20,1	15.3; 26.0	79,9	15,0	4,7	0,5	2	102; 112	18; 14	3; 7	0; 1
chr16	22,8	17.5; 29.1	77,2	15,3	6,4	1,0	2	111; 91	16; 15	7; 6	2; 0
chr17	14,6	10.4; 20.1	85,4	12,1	2,4	0,0	2	111; 95	12; 13	5; 0	0; 0
chr18	30,5	24.1; 37.7	69,5	29,9	0,6	0,0	2	92; 82	29; 23	1; 0	0; 0
chr19	42,2	34.9; 49.8	57,8	39,8	2,4	0,0	2	80; 86	36; 30	1; 3	0; 0

Synapsis and classes of asynapsis are based on the GLMM model to take into account the unequal numbers of cells analyzed per males.

Table supplement 3. Two-chr cross. The effect of the size and location of PWD/PWD conspecific intervals on asynapsis of Chr 5 and on fertility parameters.

Male ID	Distance from the centromere of Chr 5 (total length 151.8 Mb)																PWD/PWD length	Asynapsis of Chr 5		Cells analyzed	Testes weight	Sperm count
	4,9	5,2	9,8	24,5	28,1	45,0	61,4	64,1	107,0	119,0	125,4	127,0	127,7	132,1	137,7	151,0	Mb, range	%	95 % CI	N	mg	10^6
69064	PP	PP	PP	PP	PP	PP	PP	PP	PP	PP	PP	PP	PP	PP	PP	PP	151.8; 151.8	2,0	0.3; 6.0	100	54,0	0,0
69133	PP	PP	PP	PP	PP	PP	PP	PP	PP	PP	PP	PP	PP	PP	PP	PP	151.8; 151.8	2,0	0.3; 6.0	100	64,0	0,0
67974	PB	PB	PB	PB		PP	PP	PP	PP	PP	PP	PP	PP	PP	PP	PP	106.8; 123.7	0,0	0.0; 2.4	83	69,0	0,0
69083	PB	PB	PB	PB	PB		PP	PP	PP	PP	PP	PP	PP	PP	PP	PP	90.4; 106.8	1,0	0.1; 4.3	100	63,0	0,0
67730	PB	PB	PB	PB	PB		PP	PP	PP	PP	PP	PP	PP	PP	PP	PP	90.4; 106.8	0,0	0.0; 2.0	99	57,0	0,0
67878	PB	PB	PB	PB	PB	PB		PP	PP	PP	PP	PP	PP	PP	PP	PP	87.7; 90.4	1,0	0.1; 4.3	100	58,0	0,0
67882	PB	PB	PB	PB	PB	PB	PB		PP	PP	PP	PP	PP	PP	PP	PP	44.8; 87.7	2,0	0.3; 6.0	100	59,0	0,0
67876	PB	PB	PB	PB	PB	PB		PP	PP	PP		PB	PB	PB	PB	PB	54.9; 64.0	0,0	0.0; 2.0	100	69,0	0,0
69062	PB	PB	PB	PB	PB	PB	PB		PP	PP	PP	PP	PP	PP	PP	PP	44.8; 87.7	1,0	0.1; 4.3	100	58,0	0,0
67973	PB	PB	PB	PB	PB	PB	PB	PB		PP	PP	PP	PP	PP	PP	PP	32.8; 44.8	3,0	0.8; 7.6	100	67,0	0,0
69137	PB	PB	PB	PB	PB	PB	PB	PB	PB	PB	PB	PB		PP	PP	PP	19.7; 24.1	1,0	0.1; 4.3	100	55,0	0,0
69846	PB	PB	PB	PB	PB	PB	PB	PB	PB	PB	PB	PB	PB		PP	PP	14.1; 19.7	3,0	0.8; 7.6	100	NA	NA
69328	PB	PB	PB	PB	PB	PB	PB	PB	PB	PB	PB	PB	PB	PB		PP	0.8; 14.1	12,0	6.6; 19.3	100	82,0	0,0
69186	PB	PB	PB	PB	PB	PB	PB	PB	PB	PB	PB	PB	PB	PB		PP	0.8; 14.1	5,0	1.8; 10.4	100	66,0	0,0
69138	PB	PB	PB	PB	PB	PB	PB	PB	PB	PB	PB	PB	PB	PB	PB	PB	0.0; 0.0	19,0	12.1; 27.4	100	55,0	0,0
69184	PB	PB	PB	PB	PB	PB	PB	PB	PB	PB	PB	PB	PB	PB	PB	PB	0.0; 0.0	9,0	4.4; 15.6	100	74,0	0,0
69281	PB	PB	PB	PB	PB	PB	PB	PB	PB	PB	PB	PB	PB	PB	PB	PB	0.0; 0.0	11,0	5.9; 18.1	100	71,0	0,0
69331	PB	PB	PB	PB	PB	PB	PB	PB	PB	PB	PB	PB	PB	PB	PB	PB	0.0; 0.0	11,0	5.9; 18.1	100	63,0	0,0
69440	PB	PB	PB	PB	PB	PB	PB	PB	PB	PB	PB	PB	PB	PB	PB	PB	0.0; 0.0	12,0	6.6; 19.3	100	68,0	0,0
69441	PB	PB	PB	PB	PB	PB	PB	PB	PB	PB	PB	PB	PB	PB	PB	PB	0.0; 0.0	10,0	5.1; 16.9	100	71,0	0,0
69136	PP	PP	PP		PB	PB	PB	PB	PB	PB	PB	PB	PB	PB	PB	PB	9.8; 24.5	4,0	1.3; 9.0	100	61,0	0,0
69847	PP	PP	PP		PB	PB	PB	PB	PB	PB	PB	PB	PB	PB	PB	PB	9.8; 24.5	0,0	0.0; 2.0	100	NA	NA
67877	PP	PP	PP	PP		PB	PB	PB	PB	PB	PB	PB	PB	PB	PB	PB	24.5; 28.1	1,0	0.1; 4.3	100	65,0	0,0
69082	PP	PP	PP	PP	PP	PP		PB	PB	PB	PB	PB	PB	PB	PB	PB	45.0; 61.4	0,0	0.0; 2.0	100	71,0	0,0
67883	PP	PP	PP	PP	PP	PP	PP	PP		PB	PB	PB	PB	PB	PB	PB	64.1; 107.0	0,0	0.0; 2.0	100	62,0	0,0
67977	PP	PP	PP	PP	PP	PP	PP	PP	PP	PP	PP	PP	PP	PP	PP		137.7; 151.0	1,0	0.1; 4.3	100	67,0	0,0

The minimal and maximal lenght of PWD/PWD interval was determined by positions of the DNA markers used for genotyping. White and orange intervals are heterozygous PWD/B6 and homozygous PWD/PWD, respectively. Recombination breaks are located in gray intervals.

Sperm count refers to the number of sperm cells in both epididymis, TW is the wet weight of paired testes in milligrams.

Table supplement 4. Two-chr cross. The effect of the size and location of PWD/PWD conspecific intervals on asynapsis of Chr 12 and on fertility parameters.

Male ID	Distance from centromere of Chr 12 (total length 120.1 Mb)										PWD/PWD length	Asynapsis of Chr 12		Cells analyzed	Testes weight	Sperm count
	5,4	7,6	15,7	19,8	30,8	35,0	54,6	91,0	103,4	113,8	Mb, range	%	95% CI	N	mg	10^6
69064	PP	PP	PP	PP	PP	PP	PP	PP	[gray]	PB	91.0; 103.4	0,0	0.0; 2.0	100	54,0	0,0
67977	PB	PB	PB	PB	PB	[gray]	PP	PP	PP	[gray]	48.8; 78.8	0,0	0.0; 2.0	100	67,0	0,0
67876	PP	PP	PP	PP	PP	PP	[gray]	PB	PB	PB	35.0; 54.6	1,0	0.1; 4.3	100	69,0	0,0
69144	PP	PP	PP	PP	[gray]	PB	PB	[gray]	PP	PP	36.5; 59.9	1,0	0.1; 4.3	100	66,0	0,0
69760	PP	PP	PP	PP	[gray]	PB	PB	PB	PB	PB	19.8; 30.8	1,0	0.1; 4.3	100	65,0	0,0
69133	PP	PP	PP	PP	[gray]	PB	PB	PB	PB	PB	19.8; 30.8	3,0	0.8; 7.6	100	64,0	0,0
67973	[gray]	PP	PP	PP	[gray]	PB	PB	PB	PB	PB	12.2; 25.4	6,0	2.4; 11.8	100	67,0	0,0
69281	PP	PP	[gray]	PB	PB	PB	PB	PB	PB	PB	7.6; 15.7	4,0	1.3; 9.0	100	71,0	0,0
67974	PB	PB	PB	PB	PB	PB	PB	PB	PB	PB	0.0; 0.0	10,0	5.1; 16.9	100	69,0	0,0
69136	PB	PB	PB	PB	PB	PB	PB	PB	PB	PB	0.0; 0.0	9,0	4.4; 15.6	100	61,0	0,0
69138	PB	PB	PB	PB	PB	PB	PB	PB	PB	PB	0.0; 0.0	9,0	4.4; 15.6	100	55,0	0,0
69184	PB	PB	PB	PB	PB	PB	PB	PB	PB	PB	0.0; 0.0	8,0	3.7; 14.4	100	71,0	0,0
69282	PB	PB	PB	PB	PB	PB	PB	PB	PB	PB	0.0; 0.0	6,0	2.4; 11.8	100	67,0	0,0
69328	PB	PB	PB	PB	PB	PB	PB	PB	PB	PB	0.0; 0.0	12,0	6.6; 19.3	100	66,0	0,0
69331	PB	PB	PB	PB	PB	PB	PB	PB	PB	PB	0.0; 0.0	5,0	1.8; 10.4	100	63,0	0,0
69441	PB	PB	PB	PB	PB	PB	PB	PB	PB	PB	0.0; 0.0	8,0	3.7; 14.4	100	68,0	0,0
69663	PB	PB	PB	PB	PB	PB	PB	PB	PB	PB	0.0; 0.0	4,0	1.3; 9.0	100	70,0	0,0
69664	PB	PB	PB	PB	PB	PB	PB	PB	PB	PB	0.0; 0.0	8,0	3.7; 14.4	100	71,0	0,0
69847	PB	PB	PB	PB	PB	PB	PB	PB	PB	PB	0.0; 0.0	5,0	1.8; 10.4	100	63,0	0,0
69186	PB	PB	PB	PB	PB	PB	PB	PB	[gray]	PP	6.3; 16.7	10,0	5.1; 16.9	100	82,0	0,0
69763	PB	PB	PB	PB	PB	PB	PB	PB	[gray]	PP	6.3; 16.7	3,0	0.8; 7.6	100	68,0	0,0
69427	PB	PB	PB	PB	PB	PB	PB	PB	[gray]	PP	6.3; 16.7	0,0	0.0; 2.0	100	68,0	0,0
69082	PB	PB	PB	PB	PB	PB	PB	PB	[gray]	PP	6.3; 16.7	0,0	0.0; 2.0	100	71,0	0,0
69062	PB	PB	PB	PB	PB	PB	[gray]	PP	PP	PP	29.1; 65.5	2,0	0.3; 6.0	100	59,0	0,0
69083	PB	PB	PB	PB	PB	PB	[gray]	PP	PP	PP	29.1; 65.5	1,0	0.1; 4.3	100	57,0	0,0

The minimal and maximal lenght of PWD/PWD interval was determined by positions of the DNA markers used for genotyping. White and orange intervals are heterozygous PWD/B6 and homozygous PWD/PWD, respectively. Recombination breaks are located in gray intervals.

Sperm count refers to the number of sperm cells in both epididymis, TW is the wet weight of paired testes in milligrams.

Table supplement 5. Two-chr cross. The effect of the size and location of PWD/PWD conspecific intervals on asynapsis of Chr 7 and on fertility parameters

Male ID	Distance from the centromere of Chr 7 (total length 145.4 Mb)									PWD/PWD length	Asynapsis of Chr 5		Cells analyzed	Testes weight	Sperm count
	3,3	18,0	24,6	25,7	30,3	87,5	119,7	131,0	144,7	Mb, range	%	95% CI	N	mg	10^6
69468	PP	PP	PP	PP		PB	PB		PP	26.4; 44.7	4,0	1.3; 9.0	100	56,0	0,0
69745	PP	PP	PP		PB	PB	PB	PB	PB	24.6; 25.7	11,0	5.9; 18.1	100	64,0	0,0
69744	PP	PP		PB	PB	PB	PB	PB	PB	18.0; 24.6	8,0	3.7; 14.4	100	65,0	0,0
69934	PB	PB	PB	PB	PB	PB	PB	PB	PB	0.0; 0.0	10,0	5.1; 16.9	100	68,0	0,0
69935	PB	PB	PB	PB	PB	PB	PB	PB	PB	0.0; 0.0	9,0	4.4; 15.6	100	64,0	0,5
69878	PB	PB	PB	PB	PB	PB	PB	PB	PB	0.0; 0.0	8,0	3.7; 14.4	100	65,0	0,0
69627	PB	PB	PB	PB	PB	PB	PB	PB	PB	0.0; 0.0	8,0	3.7; 14.4	100	64,0	0,0
69467	PB	PB	PB	PB	PB	PB	PB	PB	PB	0.0; 0.0	7,0	3.1; 13.1	100	58,0	0,0
69626	PB	PB	PB	PB	PB	PB	PB	PB	PB	0.0; 0.0	3,0	0.8; 7.6	100	63,0	0,0
69780	PB	PB	PB	PB	PB	PB	PB	PB	PB	0.0; 0.0	1,0	0.1; 4.3	100	60,0	0,0
69572	PB	PB	PB	PB	PB	PB	PB		PP	0.7; 14.4	8,0	3.7; 14.4	100	57,0	0,0
37007	PB	PB	PB	PB	PB	PB	PB		PP	0.7; 14.4	4,0	1.2; 9.1	98	69,0	0,0
69625	PB	PB	PB	PB	PB	PB	PB		PP	0.7; 14.4	1,0	0.1; 4.3	100	65,0	0,0
69877	PB	PB	PB	PB	PB	PB		PP	PP	14.4; 25.7	1,0	0.1; 4.3	100	56,0	0,0
69781	PB	PB	PB		PP	PP	PP	PP		100.7; 119.0	3,0	0.8; 7.6	100	62,0	0,0

The minimal and maximal lenght of PWD/PWD interval was determined by positions of the DNA markers used for genotyping. White and orange intervals are heterozygous PWD/B6 and homozygous PWD/PWD, respectively. Recombination breaks are located in gray intervals.

Sperm count refers to the number of sperm cells in both epididymis, TW is the wet weight of paired testes in milligrams.

Table supplement 6. Two-chr cross. The effect of the size and location of PWD/PWD conspecific intervals on asynapsis of Chr 15 and on fertility parameters.

Male ID	Distance from centromere of Chr 15 (total length 104.0 Mb)										PWD/PWD length	Asynapsis of Chr 15		Cells analyzed	Testes weight	Sperm count
	9,3	40,0	63,0	70,2	97,0	97,8	100,6	101,9	102,8	103,4	Mb, range	%	95% CI	N	mg	10^6
69571	PP	PP		PB	PB	PB	PB	PB	PB	PB	40.0; 63.0	2,0	0.3; 6.0	100	69,0	0,0
69623	PP		PB	PB	PB	PB	PB	PB	PB	PB	9.3; 40.0	2,0	0.3; 6.0	100	65,0	0,0
69783	PB	PB	PB	PB	PB	PB	PB	PB	PB	PB	0.0; 0.0	3,0	0.8; 7.6	100	56,0	0,0
69784	PB	PB	PB	PB	PB	PB	PB	PB	PB	PB	0.0; 0.0	11,0	5.9; 18.1	100	60,0	0,0
69566	PB	PB	PB	PB	PB	PB	PB	PB	PB	PB	0.0; 0.0	13,0	7.4; 20.5	100	72,0	0,0
69469	PB	PB	PB	PB	PB	PB	PB	PB	PB	PB	0.0; 0.0	16,0	9.7; 24.0	100	56,0	0,0
69565	PB	PB	PB	PB	PB	PB	PB	PB	PB	PB	0.0; 0.0	16,0	9.7; 24.0	100	68,0	0,0
69625	PB	PB	PB	PB	PB	PB	PB	PB	PB	PB	0.0; 0.0	16,0	9.7; 24.0	100	65,0	0,0
69624	PB	PB	PB	PB	PB	PB	PB	PB	PB	PB	0.0; 0.0	19,0	12.1; 27.4	100	59,0	0,0
69746	PB	PB	PB	PB	PB	PB	PB	PB	PB	PB	0.0; 0.0	21,0	13.8; 29.7	100	62,0	0,0
69743	PB	PB	PB	PB	PB	PB	PB	PB	PB	PB	0.0; 0.0	21,0	13.8; 29.7	100	65,0	0,0
69781	PB	PB	PB	PB	PB	PB	PB		PP	PP	1.2; 2.1	24,0	16.4; 33.0	100	62,0	0,0
69878	PB	PB	PB	PB	PB	PB	PB		PP	PP	1.2; 2.1	23,0	15.5; 31.9	100	65,0	0,0
69782	PB	PB	PB	PB	PB	PB	PB		PP	PP	1.2; 2.1	16,0	9.7; 24.0	100	58,0	0,0
69879	PB	PB	PB	PB		PP	PP	PP	PP	PP	6.2; 7.0	0,0	0.0; 2.0	100	58,0	0,0

The minimal and maximal lenght of PWD/PWD interval was determined by positions of the DNA markers used for genotyping. White and orange intervals are heterozygous PWD/B6 and homozygous PWD/PWD, respectively. Recombination breaks are located in gray intervals.

Sperm count refers to the number of sperm cells in both epididymis, TW is the wet weight of paired testes in milligrams.

Table supplement 7. Two-chr cross. The effect of the size and location of PWD/PWD conspecific intervals on asynapsis of Chr 17 and on fertility parameters.

Male ID	Distance from centromere of Chr 17 (total length 95.0 Mb)										PWD/PWD length	Asynapsis of Chr 17		Cells analyzed	Testes weight	Sperm count
	4,8	15	15,6	30,9	34,7	45,4	52,7	65,3	73,8	93,2	Mb, range	%	95% CI	N	mg	10^6
64979	PB	PB	PB	PB	PB	PB	PB	PB	PB	PB	0.0; 0.0	18,8	12.0; 27.1	101	72,0	0,0
66707	PB	PB	PB	PB	PB	PB	PB	PB	PB	PB	0.0; 0.0	14,9	8.9; 22.7	101	63,0	0,0
64855	PB	PB	PB	PB	PB	PB	PB	PB	PB	PB	0.0; 0.0	14,9	8.9; 22.7	101	73,0	0,0
66954	PB	PB	PB	PB	PB	PB	PB	PB	PB	PB	0.0; 0.0	14,6	8.7; 22.3	103	71,0	0,0
64574	PB	PB	PB	PB	PB	PB	PB	PB	PB	PB	0.0; 0.0	11,7	6.5; 18.8	103	68,0	0,0
64977	PB	PB	PB	PB	PB	PB	PB	PB	PB	PB	0.0; 0.0	11,2	6.3; 17.8	116	63,0	0,0
64718	PB	PB	PB	PB	PB	PB	PB	PB	PB	PB	0.0; 0.0	12,5	6.9; 20.1	96	68,0	0,0
64849	PB	PB	PB	PB	PB	PB	PB	PB	PB	PB	0.0; 0.0	7,0	3.1; 13.0	102	76,0	0,0
66515	PB	PB	PB	PB	PB	PB	PB	PB		PP	1.8; 21.2	16,0	9.5; 24.4	92	75,0	0,0
66514	PB	PB	PB	PB	PB	PB	PB	PB		PP	1.8; 21.2	14,0	8.1; 21.7	100	71,0	0,0
64851	PB	PB	PB	PB	PB	PB	PB	PB		PP	1.8; 21.2	10,5	5.6; 17.3	105	69,0	0,0
64719	PB	PB	PB	PB	PB	PB	PB	PB		PP	1.8; 21.2	5,8	2.4; 11.3	106	62,0	0,0
66819	PB	PB	PB	PB	PB	PB	PB	PB		PP	1.8; 21.2	3,4	0.9; 8.2	100	72,0	0,0
66813	PB	PB	PB	PB	PB	PB	PB		PP	PP	21.2; 29.7	1,0	0.1; 4.2	104	68,0	0,0
66876	PB	PB	PB	PB	PB			PP	PP	PP	29.7; 42.3	0,0	0.0; 2.0	97	58,0	0,0
64575	PB	PB	PB	PB	PB		PP	PP	PP	PP	42.3; 49.6	0,0	0.0; 1.9	103	73,0	0,0
64922	PB	PB	PB	PB	PB		PP	PP	PP	PP	42.3; 49.6	2,8	0.7; 7.1	108	69,0	0,0
64975	PP		PB	PB	PB	PB	PB	PB	PB	PB	4.8; 15.0	7,9	3.7; 14.2	101	80,0	0,0
66532	PP		PB	PB	PB	PB	PB	PB	PB	PB	4.8; 15.0	6,0	2.4; 11.8	100	72,0	0,0

The minimal and maximal lenght of PWD/PWD interval was determined by positions of the DNA markers used for genotyping. White and orange intervals are heterozygous PWD/B6 and homozygous PWD/PWD, respectively. Recombination breaks are located in gray intervals.

Table supplement 8. Two-chr cross. The effect of the size and location of PWD/PWD conspecific intervals on asynapsis of Chr 18 and on fertility para

Male ID	Distance from centromere of Chr 18 (90.7 Mb)					PWD/PWD length	Asynapsis of Chr 18		Cells analyzed	Testes weight	Sperm count
	3,8	25,0	57,4	76,9	89,6	Mb, range	%	95% CI	N	mg	10^6
64574	PB	PB	PB	PB	PB	0.0; 0.0	30,8	22.5; 40.1	104	68,0	0,0
64851	PB	PB	PB	PB	PB	0.0; 0.0	21,4	14.2; 30.0	103	69,0	0,0
64719	PB	PB	PB	PB	PB	0.0; 0.0	19,3	12.7; 27.4	109	62,0	0,0
64976	PB	PB	PB		PP	1.1; 13.8	28,0	19.8; 37.3	100	71,0	0,0
66876	PB	PB		PP	PP	13.8; 33.3	9,4	3.9; 18.1	64	58,0	0,0
66877	PB	PB		PP	PP	13.8; 33.3	1,0	0.1; 4.3	101	64,0	0,0
66532	PB	PB		PP	PP	13.8; 33.3	0,0	0.0; 2.5	78	72,0	0,0
66954	PB		PP	PP	PP	33.3; 65.7	0,0	0.0; 1.9	102	71,0	0,0
66813	PB		PP	PP	PP	33.3; 65.7	0,0	0.0; 1.7	113	68,0	0,0
64922	PP	PP	PP	PP	PP	90.7; 90.7	1,8	0.3; 5.5	109	69,0	0,0
64718	PP	PP	PP	PP	PP	90.7; 90.7	0,0	0.0; 2.0	100	68,0	0,0
64975	PP	PP	PP	PP	PP	90.7; 90.7	0,0	0.0; 2.0	100	80,0	0,0
64855	PP	PP	PP	PP		76.9; 89.6	0,0	0.0; 1.9	103	73,0	0,0
64849	PP	PP	PP	PP		76.9; 89.6	0,0	0.0; 2.0	100	76,0	0,0
64575	PP	PP	PP	PP		76.9; 89.6	2,0	0.3; 6.0	101	73,0	0,0
64968	PP	PP	PP	PP		76.9; 89.6	3,0	0.8; 7.6	101	73,0	0,0
64979	PP	PP	PP		PB	57.4; 76.9	1,0	0.1; 4.3	100	72,0	0,0
66872	PP	PP	PP		PB	57.4; 76.9	2,0	0.3; 6.0	103	73,0	0,0
66514	PP	PP	PP		PB	57.4; 76.9	3,0	0.8; 7.6	100	71,0	0,0
64977	PP	PP		PB	PB	25.0; 57.4	4,8	1.7; 10.0	104	63,0	0,0
66707	PP		PB	PB	PB	3.8; 25.0	4,9	1.8; 10.2	103	NA	0,0
66815	PP		PB	PB	PB	3.8; 25.0	11,0	6.0; 17.8	109	75,0	0,0

The minimal and maximal lenght of PWD/PWD interval was determined by positions of the DNA markers used for genotyping. White and orange intervals are heterozygous PWD/B6 and homozygous PWD/PWD, respectively. Recombination breaks are located in gray intervals.

Sperm count refers to the number of sperm cells in both epididymis, TW is the wet weight of paired testes in milligrams.

Table supplement 9. Change point estimates of the minimal length [Mb] of PWD/PWD homozygosity showing detectable effect on asynapsis rate

Chr#	Experiment	[1]Change point estimate	[2]Change point lower bound	[3]Change point upper bound
Chr5	2-chr cross	19,50	14,57	24,44
Chr7	2-chr cross	[4]NA	NA	NA
Chr12	2-chr cross	20,87	6,80	34,95
Chr15	2-chr cross	8,61	-2,87	20,09
Chr17	2-chr cross	29,31	10,29	48,33
Chr18	2-chr cross	25,32	19,68	30,96
Chr15	4-chr cross	[5]2.00	0,71	3,29
Chr16	4-chr cross	12,80	8,43	17,16
Chr18	4-chr cross	33,42	10,80	56,04
Chr19	4-chr cross	19,16	12,26	26,06
Chr15	2-chr cross & 4-chr cross	7,32	1,54	13,10
Chr18	2-chr cross & 4-chr cross	27,13	21,32	32,94
Chr5,7,12,15,17,18	2-chr cross	27,14	19,36	34,91
Chr5,7,12,15-19	2-chr cross & 4-chr cross	28,40	23,18	33,63

[1]Change point estimate of the length [Mb] of PWD/PWD homozygosity in the piecewise linear regression model. For the lengths of PWD/PWD homozygosity greater than the change point, the asynapsis rate is modelled as constant.

[2]Lower bound of 95% CI.

[3]Upper bound of 95% CI.

[4]Change point cannot be determined.

[5]The estimate is influenced by two outliers with mouse ID 38759 and 38737.

Table supplement 10. Eleven G3 male parents selected for the 4-Chr cross experiment

Male ID	Chr 15 (104 Mb)					Chr 16 (98,2 Mb)						Chr 18 (90,7 Mb)					Chr 19 (61,4 Mb)				
	9,3	39,9	63,3	70.0	103,3	6,2	20,2	29,3	42,7	67,6	97.0	3,8	34.0	45,1	57,6	89,7	3,3	21,9	33.0	42,4	59,7
37487	PB	PB	PB	PB	PB	B	B	PB	PB	PB	PB	PB	PB	PB	PB	PB	PB	PB	PB	PB	PB
37504	B	PB	PB	PB	PB	PB	PB	PB	PB	PB	B	PB	PB	PB	PB	PB	B	PB	PB	PB	PB
37507	B	B	PB	PB	PB	PB	PB	B	B	B	B	PB	PB	B	B	B	PB	PB	PB	PB	PB
37715	PB	PB	PB	PB	PB	PB	PB	PB	PB	PB	PB	B	PB	PB	PB	PB	PB	PB	PB	PB	PB
37852	PB	PB	PB	PB	PB	PB	PB	PB	PB	PB	PB	PB	PB	PB	PB	B	PB	PB	PB	PB	PB
37871	PB	PB	PB	PB	PB	PB	PB	PB	PB	PB	B	PB	PB	PB	PB	PB	PB	PB	PB	PB	PB
37746	PB	PB	PB	PB	PB	PB	PB	PB	PB	PB	PB	B	PB	PB	PB	B	PB	PB	PB	PB	PB
37634	B	B	B	PB	PB	PB	PB	PB	PB	PB	PB	PB	PB	PB	PB	PB	PB	PB	PB	PB	PB
37616	PB	PB	PB	PB	PB	B	PB	PB	PB	PB	PB	B	B	PB	PB	PB	PB	PB	PB	PB	PB
37709	B	B	B	PB	PB	PB	PB	PB	PB	PB	PB	PB	PB	PB	PB	PB	PB	PB	PB	PB	PB
37862	PB	PB	PB	PB	PB	PB	PB	PB	PB	B	B	PB	PB	PB	PB	PB	PB	PB	PB	PB	B

PB - PWD/B6 heterozygosity

B - B6/B6 homozygosity

Table supplement 11. The fertility parameters of hybrids of the 4-chr cross experiment

Male ID	TW (mg)	Sperm x 10^{-6}
38754	51	0,00
38428	57	0,00
38735	58	0,00
38088	59	0,00
38089	60	0,00
38753	60	0,00
38726	61	0,00
38751	61	0,00
38755	61	0,00
38435	62	0,00
38090	63	0,00
38085	64	0,00
38087	64	0,00
38448	64	0,00
38738	65	0,00
38739	65	0,00
38711	65	0,00
38728	65	0,00
38822	65	0,00
38430	66	0,00
38432	66	0,00
38710	66	0,00
38084	67	0,00
38434	67	0,00
38814	67	0,00
38752	68	0,00
38783	68	0,00
38817	68	0,00
38758	69	0,00
38821	69	0,00
38740	70	0,00
38766	70	0,00
38813	70	0,00
38426	71	0,00
38468	71	0,00
38765	72	0,00
38767	73	0,00
38819	73	0,00
38792	74	0,00
38818	74	0,00
38820	74	0,00
38815	75	0,00
75890	68	0,00
79414	65	0,00
38712	76	0,00
38733	73	0,01
38732	63	0,01
38561	78	0,01
38713	77	0,03
38727	62	0,03
38757	72	0,04
38427	64	0,06
38429	64	0,09
38425	73	0,10
38566	63	0,17
38734	66	0,21
38086	73	0,23
38725	69	0,29
38852	75	0,34
38842	89	0,43
38759	81	0,60
38858	73	0,74
38763	81	1,02
38736	81	1,10
38764	84	1,10
38741	81	1,20
38801	83	1,51
38565	70	1,61
38794	90	1,80
38737	94	1,90
75889	90	2,10
38692	89	2,20
79415	83	2,20
38724	71	2,80
79417	90	2,80
79412	103	3,90
38433	78	4,20
38816	106	4,20
38756	85	4,70
38650	82	5,40
38652	90	5,60
38431	81	6,40
79416	95	6,40
38555	98	6,87
38793	117	10,20
75891	131	12,40
79413	108	13,70

Table supplement 12. Four-chr cross. The effect of the size and location of PWD/PWD consubspecific intervals on asynapsis of Chrs 15, 16, 18 and 19 and on fertility parameters.

Male ID	Distance from the centromere of Chr 15[1] (total length 104.0 Mb)									Asynapsis of Chr 15		Distance from the centromere of Chr 16 (total length 98.2 Mb)							Asynapsis of Chr 16		Dist. from the centromere of Chr 18 (total length 90.7 Mb)					Asynapsis of Chr 18		Dist. from the centromere of Chr 19 (total length 61.4 Mb)					Asynapsis of Chr 19		Sperm count[2]	Cells analyzed in Chrs 15, 16, 18, 19	PWD/PWD length[3] in Chrs 15, 16, 18, 19
	9,3	39,9	50,4	63,3	65,1	70,0	83,9	100,9	103,3	%	95% CI	6,2	14,0	29,3	39,1	42,7	67,6	97,0	%	95% CI	3,8	34,0	45,1	57,6	89,7	%	95% CI	3,0	21,9	33,0	42,4	59,7	%	95% CI	10^6	N	Mb, middle length
75890	PP	PP	PP	PP	PP	PP		PP	PP	1,7	0.1; 7.3	PB		PP	PP	PP	PP		1,7	0.1; 8.5	PB	PB	PB	PB	PB	20,6	13.7; 28.9	PB	PB	PB	PB	PB	24,1	14.2; 36.3	0,0	59; 45; 107; 56	104.0; 60.6; 0.0; 0.0
79414	PP	PP	PP	PP	PP	PP		PB	PB	2,1	0.3; 6.4	PB	PB	PB	PB	PB	PB	PB	16,7	10.5; 24.5	PB	PB	PB	PB	PB	28,1	17.6; 40.6	PB	PB	PB	PB	PB	26,0	17.9; 35.3	0,0	94; 108; 57; 96	77.0; 0.0; 0.0; 0.0
38435	PB	PB	PB	PB	PB	PB	PB	PB	PB	25,0	17.2; 34.0	PP	PP	PP		PB	PB	PB	4,0	1.3; 9.0	PB	PB	PB	PB	PB	39,0	29.8; 48.7	PB	PB	PB	PB	PB	33,0	24.3; 42.6	0,0	100; 100; 100; 90	0.0; 34.2; 0.0; 0.0
38087	PB	PB	PB	PB	PB	PB	PB	PB	PB	14,0	8.1; 21.7	PB	PB		PB	PB	PB	PB	11,0	5.9; 18.1	PB	PB	PB	PB	PB	18,0	11.3; 26.3	PP		PB	PB	PB	10,0	4.9; 17.3	0,0	100; 100; 100; 100	0.0; 0.0; 0.0; 12.5
38432	PB	PB	PB	PB		PP	PP	PP	PP	0,0	0.0; 2.0	PB	PB	PB	PB	PB	PB	PB	19,0	12.1; 27.4	PP	PP	PP	PP	PP	0,0	0.0; 2.0	PB	PB	PB	PB	PB	36,0	27.0; 45.7	0,0	100; 100; 100; 100	36.5; 0.0; 90.7; 0.0
38425	PP	PP	PP	PP	PP	PP		PB	PB	0,0	0.0; 2.0	PP	PP	PP	PP	PP		PB	0,0	0.0; 2.0		PP	PP	PP	PP	1,0	0.1; 4.3	PB	PB	PB	PB	PB	23,0	15.5; 31.9	0,1	100; 100; 100; 100	77.0; 55.1; 71.7; 0.0
38086	PB	PB		PP	PP	PP	PP	PP	PP	2,0	0.3; 6.0	PP		PB	PB	PB	PB	PB	4,0	1.3; 9.0	PP	PP	PP	PP	PB	1,0	0.1; 4.3	PP	PP	PP	PP	PP	0,0	0.0; 2.0	0,2	100; 100; 100; 100	47.2; 10.1; 55.3, 51.4
38759	PB	PB	PB	PB	PB	PB	PB		PP	2,6	0.4; 7.8	PB	PB	PB		PP	PP	PP	0,0	0.0; 2.0	PB	PB	PB	PB	PB	15,0	8.9; 22.8	PP	PP	PP	PP		0,0	0.0; 2.0	0,6	78; 100; 100; 100	1.9; 57.3; 0.0; 61.4
38736	PP		PB	PB	PB	PB	PB	PP	PP	4,0	1.3; 9.0	PB	PB	PB	PB	PB	PB	PB	18,0	11.3; 26.3	PB	PB		PP		8,0	3.7; 14.4	PP	PP	PP		PB	0,0	0.0; 3.0	1,1	100; 100; 100; 65	36.2; 0.0; 22.5; 37.5
38741	PP		PB	PB	PB	PB	PB	PB	PB	5,0	1.8; 10.4	PB		PP	PP	PP	PP	PP	1,0	0.1; 4.3	PP	PP	PP	PP	PP	0,0	0.0; 2.0	PB		PP	PP	PP	2,3	0.4; 6.5	1,2	100; 100; 100; 100	24.6; 76.0; 74.0, 23.0
38737	PB	PB	PB		PP	PB	PB	PB	PB	1,0	0.1; 4.3	PB	PB	PB	PB	PB	PB	PB	18,0	11.3; 26.3	PP	PP	PP	PP	PP	0,0	0.0; 2.0	PP	PP	PP	PP	PP	0,0	0.0; 2.0	1,9	100; 100; 100; 100	9.4; 0.0; 90.7; 61.4
38692	PB	PB	PB	PB	PB	PB		PB	PB	8,0	3.7; 14.4	PB	PB		PP	PP	PP	PP	0,0	0.0; 2.0	PB		PP	PP	PP	0,0	0.0; 2.0	PP	PP	PP	PP		0,0	0.0; 2.0	2,2	100; 100; 100; 100	0.0; 41.4; 51.2; 61.4
38433	PP	PP	PP	PP	PP	PP		PB	PB	0,0	0.0; 2.0	PP	PP	PP	PP	PP	PP	PP	0,0	0.0; 2.0		PP	PP	PP	PP	0,0	0.0; 2.0	PP	PP	PP	PP		0,0	0.0; 2.0	4,2	100; 100; 100; 100	77.0; 58.2; 55.0, 51.4
38756	PB	PB	PB	PB	PB	PB	PB	PB	PB	13,0	7.4; 20.5	PP	PP	PP	PP	PP	PP	PP	0,0	0.0; 2.0		PP	PP	PP		0,0	0.0; 2.0		PP	PP	PP	PP	0,0	0.0; 2.0	4,7	100; 100; 100; 100	0.0; 98.2; 74.0; 48.9
38650	PP		PB	PB	PB	PB	PB	PB	PB	2,0	0.3; 6.0	PP	PP	PP	PP	PP	PP	PP	0,0	0.0; 2.0		PP	PP	PP		0,0	0.0; 2.0	PP	PP	PP	PP		0,0	0.0; 2.0	5,4	100; 100; 100; 100	24.6; 58.2; 55.0, 11.6
38652	PB	PB	PB	PB	PB		PP	PP	PB	6,0	2.4; 11.8	PP	PP	PP	PP	PP	PP	PP	0,0	0.0; 2.0	PP	PP	PP	PP	PP	0,0	0.0; 2.2	PP	PP	PP	PP	PP	0,0	0.0; 2.0	5,6	100; 100; 91; 100	58.2; 90.7, 24.9; 53.1
38431	PB	PB	PB	PB	PP	PP		PB	PB	3,0	0.8; 7.6	PP	PP	PP	PP		PP	PB	0,0	0.0; 2.0	PP	PP	PP	PP	PP	0,0	0.0; 2.0	PP	PP	PP	PP	PP	0,0	0.0; 2.0	6,4	100; 100; 100; 100	45.1; 53.6, 51.2
38555	PP	PP		PB	PB	PB	PB	PB	PB	2,0	0.3; 6.0	PB		PP	PP	PP	PP	PP	1,0	0.1; 4.3	PB		PP	PP	PP	0,0	0.0; 2.0	PP	PP	PP	PP		0,0	0.0; 2.0	6,9	100; 100; 100; 100	51.4

[1] The minimal and maximal lenght of PWD/PWD interval was determined by positions of the DNA markers used for genotyping. White and orange intervals are heterozygous PWD/B6 and homozygous PWD/PWD, respectively. Recombination breaks are located in gray intervals.

[2] Sperm count refers to the number of sperm cells in both epididymis.

[3] The average between minimum and maximum PWD/PWD consubspecific sequence is given.

Table supplement 13. Four-chr cross experiment. The relation between observed and calculated rate of pachytene asynapsis and fertility parameters

Male ID	Testes (mg)	Sperm No x 10^{-6}	Frequency of Chr synapsed				Probability of all 4 chr synapsed	Probability of all 19 synapsed	Probability of asynaptic pachy	Obs ratio of asynaptic pachy	Obs ratio of all 19 synapsed
			15	16	18	19					
38435	62	0	0,750	0,960	0,610	0,670	0,294	0,079	0,921	0,790	0,210
38087	64	0	0,860	0,890	0,820	0,900	0,565	0,151	0,849	0,610	0,390
75414	65	0	0,979	0,820	0,719	0,740	0,427	0,114	0,886	0,660	0,340
38432	66	0	1,000	0,810	1,000	0,640	0,518	0,138	0,862	0,650	0,350
75890	68	0	0,983	0,959	0,793	0,759	0,567	0,151	0,849	0,630	0,370
38425	73	0,1	1,000	1,000	0,990	0,770	0,762	0,204	0,796	0,580	0,420
38086	73	0,23	0,980	0,960	0,990	1,000	0,931	0,249	0,751	0,360	0,640
38759	81	0,6	0,970	1,000	0,850	1,000	0,825	0,220	0,780	0,490	0,510
38736	81	1,1	0,960	0,820	0,920	1,000	0,724	0,193	0,807	0,480	0,520
38741	81	1,2	0,950	0,990	1,000	0,980	0,922	0,246	0,754	0,480	0,520
38737	94	1,9	0,990	0,820	1,000	1,000	0,812	0,217	0,783	0,400	0,600
38692	89	2,2	0,920	1,000	1,000	1,000	0,920	0,246	0,754	0,280	0,720
38433	78	4,2	1,000	1,000	1,000	1,000	1,000	0,267	0,733	0,280	0,720
38756	85	4,7	0,870	1,000	1,000	1,000	0,870	0,232	0,768	0,390	0,610
38650	82	5,4	0,980	1,000	1,000	1,000	0,980	0,262	0,738	0,360	0,640
38652	90	5,6	0,940	1,000	1,000	1,000	0,940	0,251	0,749	0,330	0,670
38431	81	6,4	0,970	1,000	1,000	1,000	0,970	0,259	0,741	0,460	0,540
38555	98	6,9	0,980	0,960	1,000	1,000	0,941	0,251	0,749	0,255	0,745

Table supplement 14. Selected SSLP markers polymorphic between B6 and PWD.

Chr No.	SSLP marker	Mbp
5	D5Mit346	4,88
5	D5Mit49	5,20
5	D5Mit178	9,83
5	D5Mit349	24,97
5	D5Mit386	28,10
5	D5Mit106	44,99
5	D5Mit302	61,43
5	D5Mit303	64,10
5	D5Mit277	107,06
5	D5Mit136	118,73
5	D5Mit138	125,10
5	D5Mit140	126,95
5	D5Mit59	127,72
5	D5Mit63	132,13
5	D5Mit326	137,43
5	D5Mit102	151,35
7	D7Mit21	3,27
7	D7Mit191	18,89
7	D7Mit180	24,63
7	D7Mit265	25,68
7	D7Mit246	30,30
7	D7Mit31	87,49
7	D7Mit66	119,89
7	D7Mit71	131,03
7	D7Mit259	144,76
12	D12Mit37	5,37
12	D12Mit215	7,61
12	D12Mit49	15,71
12	D12Mit11	22,39
12	D12Mit136	30,17
12	D12Mit147	35,72
12	D12Mit285	54,65
12	D12Mit118	91,51
12	D12Mit7	103,40
12	D12Mit20	113,36
15	D15Mit175	9,27
15	D15Mit130	20,81
15	D15Mit9	26,04
15	D15Mit138	40,03
15	D15Mit113	50,40
15	D15Mit270	63,52
15	D15Mit234	65,07
15	D15Mit67	70,20
15	D15Mit215	83,89
15	D15Mit161	97,01
15	D15Mit43	97,99
15	D15Mit97	100,80
15	D15Mit40	102,03
15	D15Mit16	102,99
15	D15Mit79	103,47
16	D16Mit55	6,24
16	D16Mit165	14,00
16	D16Mit29	20,20
16	D16Mit57	29,30
16	D16Mit12	39,12
16	D16Mit83	42,81
16	D16Mit76	67,72
16	D16Mit71	96,91
17	D17Mit19	4,81
17	D17M334	15,00
17	D17M634	15,60
17	D17Mit81	30,90
17	D17Mit33	34,74
17	D17Mit50	45,36
17	D17Mit139	52,66
17	D17Mit152	65,34
17	D17Mit93	73,80
17	D17Mit122	83,06
17	D17Mit155	84,50
17	D17Mit123	93,20
18	D18Mit66	3,84
18	D18Mit22	24,95
18	D18Mit84	33,83
18	D18Mit70	34,85
18	D18Mit149	45,00
18	D18Mit53	52,83
18	D18Mit55	53,16
18	D18Mit54	53,43
18	D18Mit124	57,46
18	D18Mit184	66,82
18	D18Mit209	66,97
18	D18Mit185	69,03
18	D18Mit7	76,85
18	D18Mit25	89,57
19	D19Mit32	3,28
19	D19Mit61	15,53
19	D19Mit128	17,25
19	D19Mit96	21,84
19	D19Mit46	32,94
19	D19Mit11	42,40
19	D19Mit71	59,60